

# ACQUIRED COLOR VISION LOSS AND A POSSIBLE MECHANISM OF GANGLION CELL DEATH IN GLAUCOMA

---

BY T. Michael Nork, MS, MD

## ABSTRACT

*Purpose:* First, to study the cellular mechanisms of acquired color vision loss in retinal detachment and diabetic retinopathy. Second, to learn why, in glaucoma, the type of color vision deficit that is observed is more characteristic of a retinal injury than it is of an optic neuropathy. Third, to test a hypothesis of photoreceptor-induced, ganglion cell death in glaucoma.

*Methods:* Various histologic techniques were employed to distinguish the L/M-cones (long/medium wavelength-sensitive cones, or red/green sensitive cones) from the S-cones (short wavelength-sensitive cones, or blue sensitive cones) in humans and monkeys with retinal detachment, humans with diabetic retinopathy, and both humans and monkeys with glaucoma. To test if the photoreceptors were contributing to ganglion cell death, laser photocoagulation was used in an experimental model of glaucoma to focally eliminate the photoreceptors. As a control, optic nerve transection was done following retinal laser photocoagulation in one animal.

*Results:* Selective and widespread loss of the S-cones was found in retinal detachment as well as diabetic retinopathy. By contrast, in human as well as experimental glaucoma, marked swelling of the L/M-cones was the predominant histopathologic feature. Retinal laser photocoagulation followed by experimental glaucoma resulted in selective protection of ganglion cells overlying the laser spots. This was not seen with retinal laser photocoagulation by optic nerve transection.

*Conclusions:* In retinal detachment and diabetic retinopathy, acquired tritan-like color vision loss could be caused, or contributed to, by selective loss of the S-cones. Both L- and M-cones are affected in glaucoma, which is also consistent with a tritan-like deficit. Although not a therapeutic option, protection of ganglion cells by retinal laser in experimental glaucoma is consistent with an hypothesis of anterograde, photoreceptor-induced, ganglion cell death.

*Tr Am Ophth Soc 2000;98:331-363*

## BACKGROUND AND HYPOTHESIS

---

Acquired color vision loss associated with retinal and optic nerve disorders has long been known to follow a somewhat predictable pattern. Retinal degeneration, regardless of the specific disease entity, often results in color confusion along a blue-yellow (tritan-like) axis, while optic nerve pathology usually produces red-green confusion. This is known as Köllner's rule.<sup>1</sup> Although similarities exist

between the acquired and congenital dyschromatopsias, the acquired disorders tend to be milder and the axis of color confusion is more diffuse.<sup>2,3</sup> In 1963, Verriest<sup>2</sup> proposed a classification system for acquired color vision defects in which he called a Type I defect the red-green confusion that is characteristic of cone degenerations, Type II the red-green defect produced by optic nerve disturbances, and Type III the blue-yellow discrimination loss seen in retinal degenerations. This system has been modified by Pokorny and associates<sup>4</sup> because the Type III defects are actually on the violet-yellow axis and, as such, are felt to be mediated by the short wavelength-sensitive cones (also referred to as S-cones, or blue cones).

Why should such a wide variety of retinal diseases produce a common color vision deficit? For instance, the observed pathologic conditions associated with glaucoma appear to be mostly confined to the inner retinal layers. Retinitis pigmentosa first involves the photoreceptors,

\*From the Department of Ophthalmology and Visual Sciences, University of Wisconsin Medical School, Madison. Supported by grant EY08724, from the National Institutes of Health, National Eye Institute; an unrestricted gift from Research to Prevent Blindness, Inc, New York, the Glaucoma Research Foundation, San Francisco, the Wisconsin Lions Eye Research Fund, Stevens Point; and the Steve J. Miller Foundation, Marshfield, Wisconsin. Some of the work in this thesis was done at the Department of Ophthalmology, West Virginia University School of Medicine, Morgantown.

especially those in the mid-periphery. With cystoid macular edema and macular degeneration, the pathology is localized in the macula. Diabetes mellitus damages the entire retina, including all retinal layers in both the macula and periphery. Is there a common underlying disorder in the blue-sensitive pathway with all of these diseases? Or do different diseases affect different levels of the pathway? Finally, what would make the S-pathway more susceptible than the L- and M-(long and medium wavelength, or red and green) pathways?

#### *Etiology of Acquired Color Vision Loss*

Despite the considerable number of studies confirming the validity of Köllner's rule for retinal degenerative diseases, there is little direct evidence to suggest an underlying etiology. The following is a review of the major hypotheses.

*Filtering.* A Type III color deficit can result from simple filtering of the short wavelengths. Wearing amber-colored sunglasses would be a trivial example of this. A similar phenomenon occurs with brunescient (nuclear sclerotic) cataracts. Vitreous filtering from old blood, yellowish subretinal fluid (in serous and rhegmatogenous retinal detachments) and changes in intraretinal pigment (xanthophyll, blood, exudates, intraretinal migration of retinal pigment epithelium) have also been proposed as mechanisms for short-wavelength filtering in various retinal disorders.<sup>5-7</sup>

Köllner's rule, as it applies to retinal disease, has great generality (ie, almost every retinal degenerative disorder has now been shown to produce a Type III defect). Guided by Ockham's razor, one might predict an etiology with similar generality. The filtering hypothesis requires many types of filters to explain a single phenomenon. For example, young people with retinitis pigmentosa (RP) do not have brunescient cataracts, central serous retinopathy is not associated with intraretinal pigmentary changes, diabetic retinopathy can produce blue color deficits prior to ophthalmoscopically observable retinal changes,<sup>8,9</sup> drugs [eg, digitalis, sildenafil [Viagra]<sup>10,11</sup>) produce no known morphologic changes.

*Paucity of S-cones.* The relative scarcity of the S-cones may be sufficient to explain selective loss of blue sensitivity with disease. However, if the receptor system is linear, losing an equal percentage of all 3 cone types would have no effect on color discrimination.<sup>12</sup> But it may be that there are so few S-cones that there is little overlap between adjacent receptive fields so that losing even a small percentage would result in large gaps in the S-cone matrix.<sup>13,14</sup>

*Limited Response Range of S-cones.* A Type III defect could occur without an actual loss of photoreceptors. It has been observed that the luminance response range of

the S-cones is narrower than for the L- and M-cones.<sup>12,15-16</sup> If a disease were to result in the response ranges for all 3 types to drop proportionately, the S-cones might saturate while the L- and M-cones would maintain some sensitivity.

*Heterogeneity in Effect of Retinal Disease.* Hart and coworkers<sup>17-19</sup> argue that the unequal distributions of S- and L/M-cones could account for Köllner's rule. The L/M-cones increase in density with decreasing foveal eccentricities; achieving a sharp maximum in the foveal center.<sup>20</sup> The S-cones reach their greatest density within 1 or 2 arc degrees of retinal eccentricity from the foveal center. With smaller eccentricities, their numbers fall precipitously and they may even be absent within 8 arc minutes of the center.<sup>20-26</sup> If retinal disease were to preferentially affect the parafoveal region (where S-cones are at their greatest concentration) and spare the fovea itself, a much greater percentage of S-cones would be injured. A Type III defect would then result.

Some conditions, such as the paracentral and arcuate scotomas of glaucoma, the ring scotoma of RP, the "bull's-eye" maculopathy of chloroquine retinopathy do seem to fit this pattern. But others, such as retinal detachment, diabetic retinopathy, central serous retinopathy, and age-related macular degeneration do not obviously spare the fovea. Silverman and associates<sup>27</sup> have compared the particular pattern of color vision deficit and the spatial distribution of visual field loss in individuals with optic neuritis and diabetic retinopathy and found a good correlation in optic neuritis but no significant association for diabetic retinopathy.

*Selective Cone Fragility.* The S-cones (or their associated higher-order neurons) might simply be more susceptible to stress than the L- or M-cones. Such a hypothesis is not unreasonable considering the fundamental biochemical and genetic differences that exist between S-cones and L/M-cones.

Indirect evidence exists for this premise. de Monasterio and colleagues<sup>23, 24, 28</sup> proposed that their observation of S-cone staining with several different vital dyes could be explained on the basis of a selectively greater toxic effect of the dyes to the S-cones (for example, see Fig 1). Zrenner and Gouras<sup>29</sup> speculated that there may be morphologic differences in the outer segments of the S-cones and L/M-cones such that the former are less efficient at handling certain metabolites.

Alternatively, it might be that the L/M-cones are more easily damaged than the S-cones. If the L- cones and M-cones are affected almost equally, then according to the concept of color opponency, blue-yellow confusion would ensue, since the sum of equal red and green stimuli produce the sensation of yellow.<sup>30-32</sup> That the L- and M-cones should be affected nearly equally by various retinal disease processes is not an unreasonable

assumption considering the 96% homology of their opsins, compared with only a 43% similarity with S-cone opsin,<sup>33</sup> as well as other biochemical similarities as suggested by their similar histochemical staining patterns with opsin antibodies<sup>34,35</sup> and with antibodies to the various S-antigen isoforms.<sup>36</sup> Indeed, recent work by Greenstein and associates<sup>37</sup> with increment threshold color opponency testing suggests that in glaucoma, the defect may be mostly red-green, while in diabetes it is predominantly blue sensitivity loss.

Selective fragility may involve the cones or postreceptoral color pathways, or both. In RP, for example, an electrophysiologic and psychophysical study suggests that actual cone loss occurs.<sup>38</sup> This has been supported by the finding of S-cone opsin but little L/M-cone opsin in one patient with dominant RP.<sup>39</sup> (Nondominant RP may have reduced S-cone acuity.<sup>40</sup>) On the other hand, Greenstein and coworkers<sup>41</sup> have found psychophysical evidence for postreceptoral sensitivity loss in diabetes.

Data in the following 3 sections support this hypothesis of selective cone fragility.

#### **S-CONE LOSS IN RETINAL DETACHMENT**

(The material in this section involving human retinal detachment has been previously published. The data on experimental detachment have not been published, except in abstract form.)

##### *Introduction*

Color vision deficits associated with retinal detachment have been known since the early part of the 20th century. In 1907, Köllner<sup>42</sup> examined 36 affected patients, 32 of whom showed a blue-yellow (tritan-like) discrimination deficit. Subsequent efforts by several groups have now confirmed that blue-yellow confusion is the most commonly acquired color vision defect in retinal detachment but that, as is typical of acquired color vision loss, the deficit is not always a pure one.<sup>5,43-46</sup> Marré agreed that a blue-yellow loss was associated with detachment but believed that the blue mechanism was most severely affected<sup>45</sup> (ie, representing a Type III defect as revised by Pokorny and colleagues<sup>4</sup>). Recovery of the retina after detachment repair has also been examined.<sup>44</sup> The color vision defects were observed whether or not the macula was initially detached, but when it was, the color deficit was more severe and recovery was slower and incomplete. Recovery of color vision also tended to be incomplete after macular detachments.

Rhegmatogenous retinal detachment is an interesting disorder from a histopathologic standpoint because its onset is acute and there is usually no associated retinal pathology other than a peripheral tear. Furthermore, the

possible etiologic mechanisms for retinal degeneration are limited to either ischemia or interruption of the interface between the photoreceptors and retinal pigment epithelium (RPE). Ischemia is only partial and involves mainly the outer retinal layers (including the photoreceptors). It results from the physical separation of the neurosensory retina from the choroidal circulation. Recovery from ischemia is possible, as evidenced by the often dramatic improvement in Snellen visual acuity following surgical reattachment<sup>47-49</sup> and by the re-formation of the outer segments seen in animal models,<sup>50-52</sup> but the healing is incomplete. The final visual acuity is dependent on the duration of the macular detachment prior to repair, but seldom do patients regain 20/20 vision, even with detachments of 1 day or less.<sup>47,49</sup> This may be due to a failure to fully reestablish the photoreceptor/RPE interface.<sup>47,49,52</sup> One might not, a priori, expect either of these mechanisms of damage (ischemia or disruption of photoreceptor/RPE interface) to selectively affect a particular population of photoreceptors, since they all are involved in both processes. Therefore, if relatively greater morphologic injury to one cone type could be demonstrated, then the hypothesis of differential cone fragility as a cause of color vision loss would be strongly supported.

This question was previously addressed by Nork and associates<sup>53</sup> in a histopathologic study of 10 human eyes with traumatic rhegmatogenous retinal detachment. Eight of the eyes were removed from 2 1/2 to 11 days following trauma. In the remaining 2, the retinas were successfully reattached. Enzyme histochemistry for carbonic anhydrase (CA) and immunocytochemistry for S-antigen were performed to distinguish S-cones from L/M-cones.

With the 2 1/2-to 4-day-old detachments, nearly all of the CA-negative cones (S-cones) and many of the rods were seen to have signs of irreversible necrosis, including extreme swelling of the inner segments and mitochondria, loss of the outer segments, and pyknotic and displaced nuclei. In the 6- and 11-day detachments, almost all of the CA-negative cones and many rods were missing. S-cones were essentially absent from the reattached retinas, and there were only about half the normal number of rods (Fig 2).

The following sections describe further histopathologic investigations involving experimental rhegmatogenous detachment in monkey and serous detachment associated with choroidal melanoma in human.

##### *Methods*

All of the animal investigations described in this thesis conformed to the Association for Research in Vision and Ophthalmology (ARVO; Rockville, Maryland) statement on the use of animals in vision research, and approval was obtained from the relevant animal care and use committees.

Two rhesus monkeys were studied. Monkey 1 underwent a vitrectomy, including removal of the posterior hyaloid, followed by injection of 0.1 mL of saline under the superior retina. A large retinotomy was made. The retina spontaneously reattached within 2 days. On the same eye, 0.1 mL of perfluorooctane (PFO) was then injected beneath the inferior retina. This produced a large, inferior detachment. The eye was enucleated 22 days later. Monkey 2 had a vitrectomy with removal of the posterior hyaloid as well. This time, only 0.075 mL of PFO was injected under the retina just superior to the superotemporal arcade vessels. Within 4 days, a subtotal retinal detachment and giant dialysis formed (Fig 3). After 2 weeks, retinal reattachment was attempted by applying an encircling scleral buckle, removing the PFO, and performing a gas-fluid exchange (15% C<sub>3</sub>F<sub>8</sub>). Although the retina was attached for about 1 month, it redetached following resorption of the C<sub>3</sub>F<sub>8</sub>. The animal was sacrificed 2 months after the initial procedure so the total time of detachment was about 1 month.

Twenty-four hours prior to enucleation, both eyes of each monkey were injected intravitreally with Lucifer yellow. Following fixation in paraformaldehyde, segments of retina were embedded in glycol methacrylate and sectioned. Lucifer yellow is a vital dye known to specifically label the cell bodies of the S-cones in rhesus monkey (it also labels all cone, but not rod, outer segments).<sup>23</sup>

### Results

As in the human traumatic retinal detachments, the surgically induced detachments in the monkeys resulted in near total loss of Lucifer yellow staining. This was true in both the peripheral (Fig 4) and the macular retina (Fig 5).

### Conclusions.

Although it could be argued that the S-cones change their staining characteristics following retinal detachment, this would not explain the progression of events, beginning with swelling and eventual absence of the CA-negative cones in the human study. In addition, a few CA-negative cones survived, and these showed immunoreactivity for the same isoform of S-antigen as seen in the S-cones in control retinas.

No early detachments were examined in the monkeys, so the possibility that the detachment simply reduced the uptake of Lucifer yellow cannot be ruled out. However, as in the humans, this would not explain why a few of the cones were strongly positive. Because there was not gradient of dye uptake, a reasonable interpretation is that after 2 weeks, most of the S-cones had degenerated. Furthermore, the results are consistent with the S-cone loss seen in the humans.

Such a selective loss of nearly all of the S-cones would

certainly explain the blue-yellow color deficits found in retinal detachment. Beyond that, however, these findings are interesting for a number of reasons. For one thing, why are the S-cones (and to a lesser extent the rods) so susceptible to injury in retinal detachment? Although the present study does not address this question, it could be speculated that the comparative resistance of the L/M-cones has something to do with their intracellular CA. Because the enzyme histochemical technique recognizes all of the various isoenzymes of CA, it is reasonable to assume that the S-cones and rods have either no, or very low levels of, intracellular CA. Yet they may still require this enzyme for such things as the maintenance of intracellular pH and fluid transport. Donner and associates<sup>54</sup> propose that the rods benefit from the abundant CA found in the adjacent Müller's cells and the RPE. In retinal detachment, however, the rods and S-cones lose contact with the RPE and its stores of CA. Exacerbating the situation, within hours of a retinal detachment the Müller's cells show a dramatic decrease in their production of CA and a concomitant increase in synthesis of intermediate filaments such as glial fibrillary acidic protein and vimentin<sup>55</sup>—a condition that persists in chronic detachment.<sup>56</sup> The L/M-cones continue to label strongly for CA even when the retina is detached. This independent source of CA may serve a protective role against the pH changes related to ischemia or against the effects of edema.

Carrying this argument a step further, the greater fragility of S-cones compared to the rods may relate to their baseline metabolic activity. Cones have larger inner segments, containing greater numbers of mitochondria than rods. Presumably, these mitochondria are there to support higher energy needs associated with processing large numbers of captured photons under photopic conditions. If the S-cones are more active than the rods, they may also be more easily injured by ischemic stress.

### S-CONE LOSS IN DIABETIC RETINOPATHY

#### Introduction

A range of disorders is ophthalmoscopically evident in diabetic retinopathy. Mild, or "background," changes include capillary microaneurysms, hard exudates, small intraretinal hemorrhages and cotton-wool spots (swellings of the axons of the nerve fiber layer). More advanced, or "proliferative," defects are composed of capillary dropout and intraretinal microangiopathy (IRMA). Finally, severe abnormalities, such as extraretinal neovascularization, periretinal membrane formation with retinal traction detachment, and vitreous hemorrhages, are seen in the "proliferative" form of the disease. Panretinal laser photocoagulation has been found to be of benefit in preventing

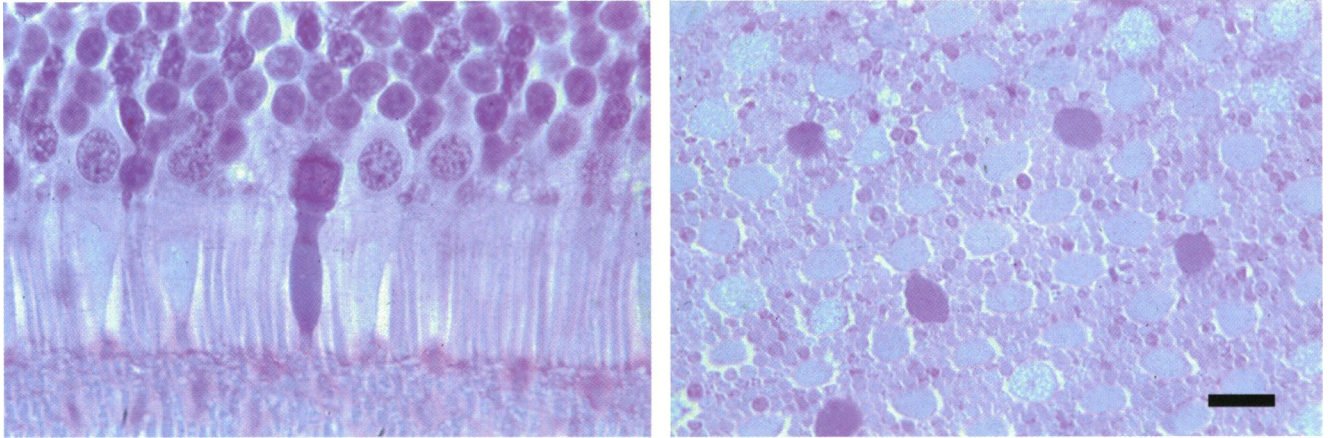


**FIGURE 1**

Sections of retina from rhesus monkey whose vitreous had been injected 24 hours prior to enucleation with vital dye, procion black. Left, Radial section showing single labeled cone (dark blue) among others that are unstained. Right, Same retina sectioned tangentially to surface of globe (parallel to plane of retina) at level of photoreceptor inner segments. About 10% of cones are labeled. Labeled cones are evenly distributed among dominant cone population (toluidine blue counterstain; bar = 10  $\mu$ m).

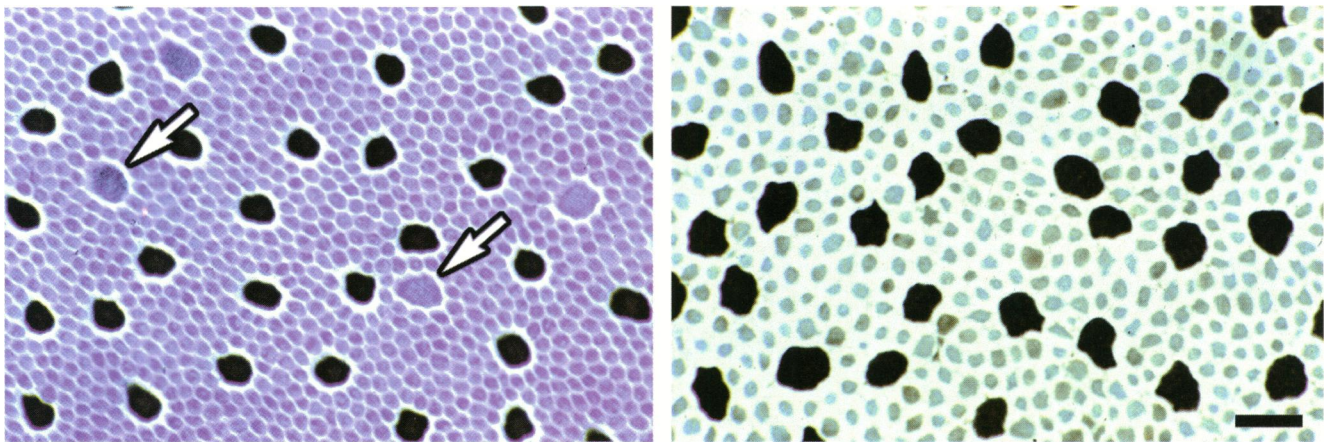


**FIGURE 2**

Tangential sections of retina, enzyme histochemical reaction for carbonic anhydrase (CA, black reaction product), which is known to label L/M-cones but not S-cones or rods. Left, Control retina. CA-negative cones are present (arrows). Right, Subject with surgically reattached retina. Note absence of CA-negative cones. About half as many rods are present as seen at left. (toluidine blue counterstain; bar = 10  $\mu$ m). Contrast and brightness were adjusted digitally.

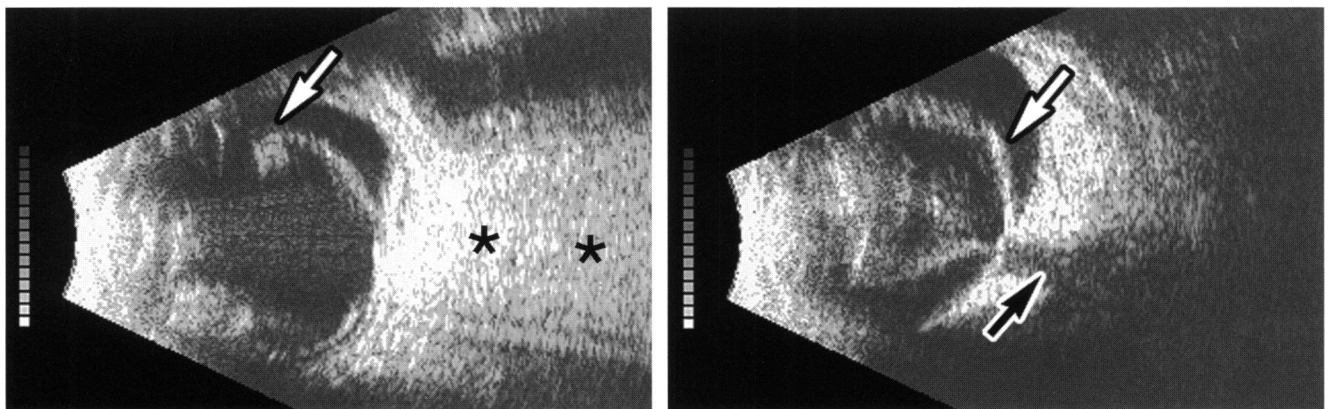


**FIGURE 3**

B-scan ultrasonogram of monkey No. 3, 2 weeks following vitrectomy and subretinal injection of perfluorooctane (PFO). Left, With head supine, superior leaf of detached retina is readily visible. Anterior end of retina is inverted, a characteristic of giant tears (arrow). Note multiple inter echoes (so called "ringing") generated by subretinal PFO (asterisks). Right, With head held upright, PFO has moved out of field of ultrasonic beam and shadow corresponding to optic nerve is visible (black arrow). Echoes corresponding to V-shaped subtotal retinal detachment are evident (white arrow).

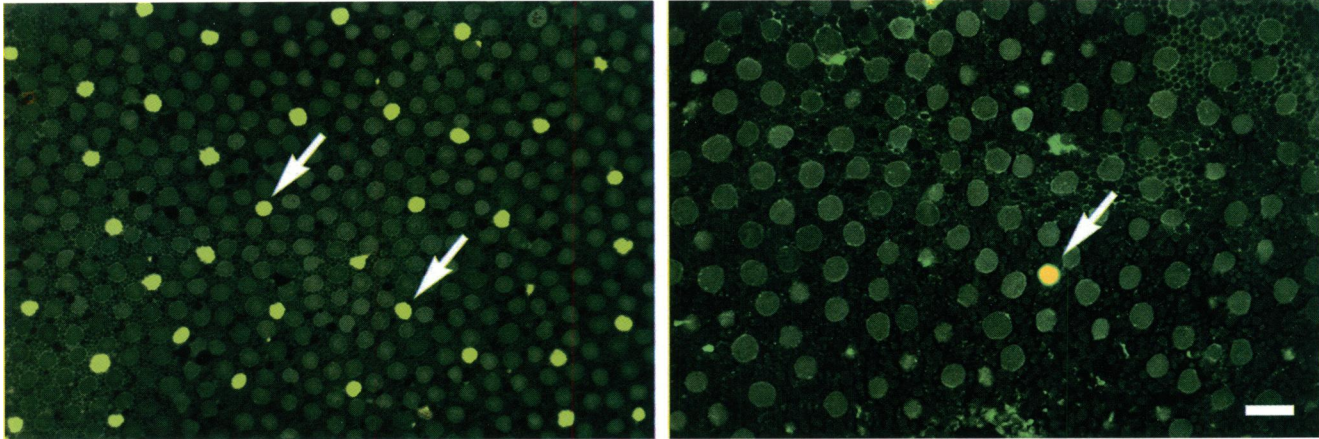


FIGURE 4

Fluorescent microscopy of midperipheral retina of rhesus monkeys. Left, Retinal section from unoperated, control eye. Although it is of midperipheral retina, it is slightly closer to macula than retina shown on right. Lucifer yellow-labeled cones (arrows) make up about 10% of total cone population. Rods (difficult to see on this image) are also more plentiful than in detached retina. Right, Tangential section of retina at level of photoreceptor inner segments of monkey No. 1 with 2-week-old detachment. Only rare cones label with Lucifer yellow (arrow). Labeled cones make up 0.7% or less of total cone population in detached retina. Contrast, brightness, and hue were adjusted digitally.

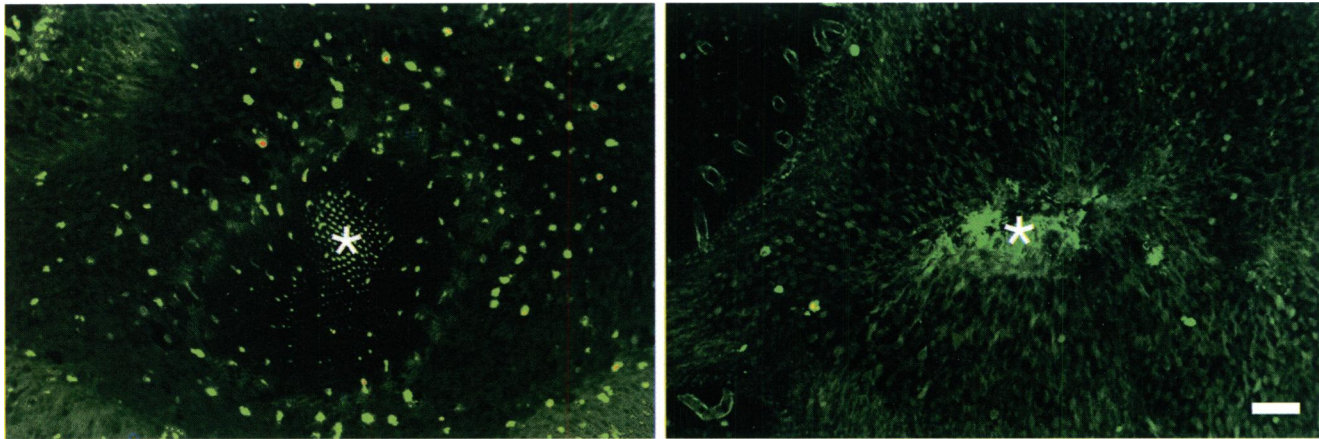


FIGURE 5

Fluorescent microscopy of central maculae of monkey No. 2. Left, Unoperated fellow (control) eye. Numerous Lucifer yellow-positive cones are evident (bright yellow dots). Due to natural curvature of tissue, section passes through outer segments in central fovea (asterisk), which are positively labeled in all cones. Right, Tangential section of experimental eye in which retina had been detached for a total of about 1 month and remained detached at time of enucleation. Foveal center is marked with asterisk. Only rare cones are positive for Lucifer yellow. Note that in central fovea, section passes through detached cone outer segments, all of which are labeled. Contrast, brightness, and hue were adjusted digitally.

visual loss in many patients with proliferative changes.<sup>57</sup>

As with other retinal degenerative processes, the characteristic pattern of color vision loss in diabetic retinopathy is of the tritan-like, or Verriest Type III variety.<sup>2</sup> This selectivity of damage for the S-cone pathway was further demonstrated by Adams and colleagues,<sup>58</sup> who measured the spectral sensitivities for each of the 3 cone pathways in patients with diabetic macular edema. They found that the S-pathway was 40 times less sensitive than in normal controls, compared with the L- and M-pathways, which were only 2.2 times less sensitive. More recently, Greenstein and coworkers<sup>37,59,60</sup> have carefully measured S-cone pathway sensitivity using an increment threshold technique and found the S-cone pathway to be

specifically affected in diabetes. The L- and M-cone pathways showed less sensitivity loss. The rods seem to be less sensitive in diabetes, as well.<sup>61,62</sup>

Tritan-like defects have been found in all stages of diabetic retinopathy. Kinnear and associates<sup>8</sup> and Lakowski and colleagues<sup>9</sup> studied 549 patients with diabetes, most of whom had mild or no apparent retinopathy, and found that despite normal visual acuity in most patients, color vision loss was common. More recent studies have confirmed the presence of Type III loss even in patients with ophthalmoscopically absent or minimal retinopathy.<sup>8,63-65</sup> Some controversy exists as to the correlation of the color defect with severity of the retinopathy. Kinnear and coworkers<sup>8</sup> found that at all ages

studied (group averages of 25 to 65 years old in 10-year increments), the color vision loss was worse in those subjects with at least some retinopathy. Moloney and Drury<sup>66</sup> studied 66 young patients with diabetes (mean age, 27.7 years) and did not observe a relationship between stage of the disease and magnitude of the color vision loss. Bresnick and associates,<sup>67</sup> on the other hand, examined 90 patients with diabetes (both young and old) and concluded that the magnitude of the acquired tritan-like discrimination loss was correlated significantly with both the severity of the overall diabetic retinopathy and the severity of macular edema and hard exudate formation. An independent risk factor for tritan-like color vision loss seems to be the application of panretinal laser photocoagulation,<sup>68-70</sup> even though the macula is avoided in this treatment.

A question has arisen as to whether the tritan-like deficit in diabetes is prereceptor, receptor, or postreceptor. In support of a prereceptor mechanism, Lutze and Bresnick<sup>71</sup> found that the lenses in patients with diabetes "yellow" at an accelerated rate. However, they later found that when correcting for these lens changes, areas of reduced S-cone system sensitivity were present. Using blue test spots on a bright yellow background, Terasaki and colleagues<sup>72</sup> concluded that the pattern of sensitivity loss cannot be caused by changes in preretinal screening. Even so, Tregear and coworkers<sup>73</sup> employed chromatic-contrast threshold testing and concluded that, the specific tritan deficits seen in patients with diabetes can be explained by lens yellowing rather than by selective damage to the S-cone system. Further complicating matters, Greenstein and associates<sup>41</sup> found psychophysical evidence for postreceptor sensitivity loss in patients with diabetes. Holopigian and colleagues<sup>74</sup> used 2-color dark-adapted thresholds, as well as electrophysiologic testing, and concluded that there were rod and cone receptor as well as postreceptor deficits.

Considering our previous results showing selective loss of S-cones in human retinal detachment,<sup>53</sup> we wanted to determine if a similar pathogenic mechanism was involved in diabetic retinopathy, which might explain the observed color vision loss in this disease. Two methods were used to accomplish this goal. First, to allow a qualitative assessment of cell death, retinal tissue was labeled using the terminal deoxynucleotidyl transferase (TdT)-mediated biotin-deoxyuridine triphosphate (dUTP) nick end labeling (TUNEL) method. Second, a quantitative analysis comparing densities of S-cones as well as L/M-cones was conducted. Because of the great biochemical similarity of the L/M-cones, no convenient method has been developed to distinguish these 2 cone types in post mortem tissue. However, the technique of enzyme histochemical analysis for CA described in the following section is a rapid method for distinguishing the S-

cones (CA-negative) from the L/M cones (CA-positive) in human eyes, so long as too much autolysis has not occurred.

### *Methods*

The experiments described in this section followed the tenets of the Declaration of Helsinki and were approved by the appropriate institutional review board.

*TUNEL Procedure.* Portions of 5 retinas from 5 subjects with varying degrees of diabetic retinopathy (subjects D1, D5, and D7 [Table I]) plus 2 additional eyes from 2 subjects that were not used for the quantitative study described here and 1 postmortem control eye (without known retinal disease) were embedded in paraffin. Putatively apoptotic nuclei were labeled by the TUNEL method.<sup>75,76</sup> Paraffin sections (4  $\mu$ m thick) were mounted on slides treated with adhesive (Vectabond, Vector Laboratories, Burlingame, California) deparaffinized, and rehydrated with distilled water. All sections were digested with proteinase K and blocked for endogenous peroxidase. TdT was used to incorporate biotinylated dUTP at the sites of DNA breakdown. Biotinylated dUTP was visualized with streptavidin and diaminobenzidine (DAB). Rat small intestine with and without DNase added before incubation in TdT and biotin-dUTP served as positive controls. Negative controls were incubated without biotin-dUTP.

*Labeling of L/M-cones for CA.* Postmortem retinas were obtained from 13 human donors, 7 from patients with various durations and stages of diabetic retinopathy (D1 through D7, Table I) and 6 controls. The tissue was fixed in 4% phosphate-buffered paraformaldehyde (pH, 7.2) for 24 to 48 hours at 4° C and then stored in 1% phosphate buffer (pH, 7.4) at 4° C. Representative pieces of retina were removed and embedded in glycol methacrylate (GMA; JB-4, Polysciences Inc, Warrington, Pennsylvania). To preserve enzyme activity, the tissue was embedded directly in GMA without the usual dehydration in graded alcohols. Instead, the specimens were gently agitated in graded concentrations of GMA monomer with benzoyl peroxide catalyst and distilled water, beginning with a 1:1 mixture. Polymerization was carried out at 0° C for 16 hours. Sections were cut 2  $\mu$ m thick with the tissue oriented either radially or tangentially to the plane of the retina, and reacted for CA according to a modified version<sup>26, 77</sup> of the Hansson method.<sup>78,79</sup> This involved floating the tissue sections on the surface of a reacting medium consisting of 0.00715 M CoSO<sub>4</sub>, 0.0526 M H<sub>2</sub>SO<sub>4</sub>, 0.0117 M KH<sub>2</sub>PO<sub>4</sub>, and 0.157 M NaHCO<sub>3</sub> for 4 to 8 minutes. The sections were rinsed by floating them on a 0.5% solution of (NH<sub>4</sub>)<sub>2</sub>S for 1 minute and rinsing again on distilled water. They were mounted on glass slides and counterstained with toluidine blue.

*Quantitative Analysis.* The tissue sections were viewed with a microscope (Olympus BH-2; Olympus

TABLE I: CLINICAL BACKGROUND OF SUBJECTS AND CONTROLS

	AGE (YEARS)	SEX	DET (HOURS)	FIXATION (DAYS)	CD	VA	STAGE	LASER	DURATION (YEARS)
Subjects									
D1	65	M	20(ice)	2	CVA	0.5	PDR	PRP	13
D2	67	M	4.5	2	Cardiac arrest	0.1	BDR	None	20
D3	69	F	NA	NA	NA	0.5	BDR	None	NA
D4	68	M	5	7	GI bleed	NA	PDR	PRP/ML	NA
D5	68	F	2.5	4	NA	0.02	PDR	PRP	24
D6	62	F	12	NA	NA	NA	PDR	None	30
D7	66	M	4	4	NA	NA	BDR	None	8
Controls									
C1	74	F	2.5	5	MI				
C2	12	M	0.5	3	Head trauma				
C3	66	F	2	22	CHF				
C4	40	M	NA	NA	Liver cirrhosis				
C5	68	F	2	2	Breast cancer				
C6	68	F	1.4	1	Cardiac arrest				

BDR, background diabetic retinopathy; CD, cause of death; CHF, congestive heart failure; CVA, cerebrovascular accident; DET, death to enucleation time (D1 was kept on ice prior to fixation, the other eyes were at room temperature); DM, diabetes mellitus; GI, gastrointestinal; MI, myocardial infarction; ML, macular laser; NA, information not available; PDR, proliferative diabetic retinopathy; PRP, panretinal photocoagulation; VA, visual acuity.

Corporation, Lake Success, New York) and a digital camera (Sony 3-chip charge-coupled device [3CCD], Model DXC 960 MD, Sony Medical Systems, Montvale, New York). The digital image was then captured and densities of the 2 cone-types (CA-positive and CA-negative) were measured using image analysis software (Optimas, Media Cybernetics LP, Bothell, Washington).

The location of any point on the retina can be specified by 2 coordinates: the distance from the fovea and the degree from the temporal meridian (ie, the 3-o'clock meridian for left eyes, the 9-o'clock meridian for right eyes). At 100  $\mu\text{m}$ , 1 point was sampled every 45° (8 points); at 150  $\mu\text{m}$ , every 30° (12 points); and at 200  $\mu\text{m}$ , every 22.5° (16 points). Beyond 200  $\mu\text{m}$  up to 1.5 mm, data were collected every 45° (8 points) at 200  $\mu\text{m}$  intervals (Fig 6). A modification of the method of Curcio and coworkers<sup>30</sup> was used to create a smooth tessellation of the central retina—producing 2-D topographical maps.

A method similar to that described by de Monasterio and associates<sup>24</sup> was employed for the peripheral retina. Cone topography was determined by sampling 360° (as described above) from 100 to 1,500  $\mu\text{m}$  of retinal eccentricity (distance from the foveal center) and then along the horizontal meridians from 3 to 15 mm. Four points were sampled near the horizontal meridian beyond 1.5 mm. All of the data for each eccentricity, regardless of direction, were then averaged (Fig 7). (The distances as given do not account for tissue shrinkage, which is about 15% for embedment in GMA. To convert millimeters to degrees of retinal eccentricity for the average adult eye, assuming

15% shrinkage, a factor of 3.96 %/mm should be used.)

It was not possible to include all points at every eccentricity, primarily because of weak staining reaction or tissue folding. CA enzyme histochemical method is very sensitive to autolysis and fixation. In some locations of some eyes, the reaction was too weak to distinguish CA-positive from CA-negative cones. Tissue folding during

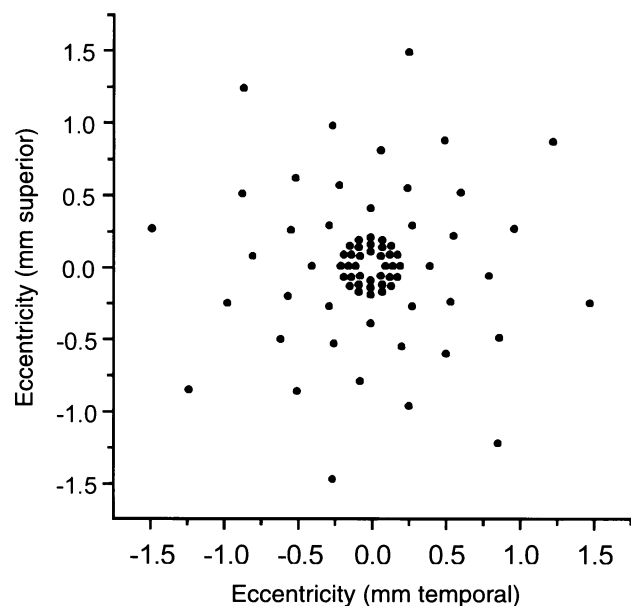


FIGURE 6

Locations of sampling points for retinal eccentricities (distances from foveal center) from 100  $\mu\text{m}$  to 15 mm.



embedding presented occasional problems as well, making it difficult to obtain sections that were flat enough for adequate sampling. The central fovea (0 and 50  $\mu\text{m}$  eccentricity) presented its own technical difficulties when this technique was employed. CA staining was particularly weak in this region—only yielding usable results in a few eyes. Also, the retina was thinner here so that, during fixation and embedding, tissue shrinkage caused the photoreceptor layer to move vitreally—producing a concave outer surface opposite the fovea interna. Because of this, tangential sections through the fovea were generally not flat enough for analysis. Given these problems and the normal paucity of S-cones in the central fovea, statistical comparisons between diabetic retinopathy and control eyes are not meaningful for eccentricities of less than 100  $\mu\text{m}$  with the use of this technique.

### Results

Occasional nuclei were found to be TUNEL-positive in all of the 5 diabetic retinas tested, but not in the controls. Positive cells were found in the both the inner and outer nuclear layers. In 1 case, a positively labeled nucleus (possibly from a cone<sup>53</sup>) was seen that was external to the outer limiting layer (Fig 8).

Unlike the controls, the diabetic eyes showed patchy losses of CA-negative cones (presumably S-cones) and rods (Fig 9). On average, there was reduction in the percentage of S-cones in all directions and at all eccentricities in the maculae of the diabetic eyes compared with the

control eyes (Fig 10). However, for individual eyes, these losses were sometimes irregular (Fig 11). A significantly lower density of S-cones was found at nearly all retinal eccentricities from 0.1 to 15 mm (Fig 12). By comparison, the mean density of L/M-cones was significantly reduced at only 1.5mm (Fig 13).

Since the S-cones normally have a regular distribution with respect to the L/M-cones,<sup>24,53</sup> we reasoned that measuring the ratio of S-cone to L/M-cone densities would be a sensitive measure, since, being a ratio, it would compensate for artifacts such as irregular tissue shrinkage during embedding. Thus as shown in Fig 14, the S-cones, as a percentage of all cones, were significantly reduced in the diabetic eyes at all but 3 eccentricities. On average, the percentage of S-cones compared to L/M-cones was decreased by  $21.0 \pm 3.4\%$  (mean  $\pm$  SEM) in the eyes with diabetic retinopathy compared with controls.

### Conclusions

Selective dropout of S-cones is a consistent finding in diabetic retinopathy. The loss is, on average, distributed rather evenly throughout the macula and along the horizontal meridian, extending at least to 15 mm beyond the fovea. Selective S-cone injury is similar to (although less extensive than) what is seen in retinal detachment,<sup>53</sup> but contrasts with the L/M-cone damage found in glaucoma.<sup>51</sup>

An effort was made to select eyes with a range of diabetic retinopathy. However, because complete ocular histories were not available for all patients and because of the

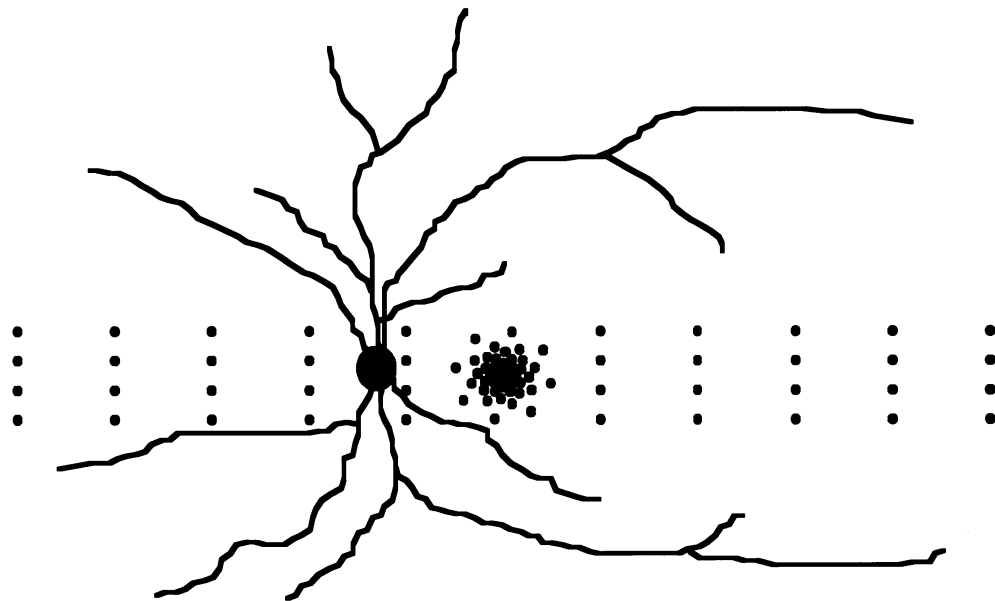


FIGURE 7

Locations of sampling points for retinal eccentricities up to 15 mm.

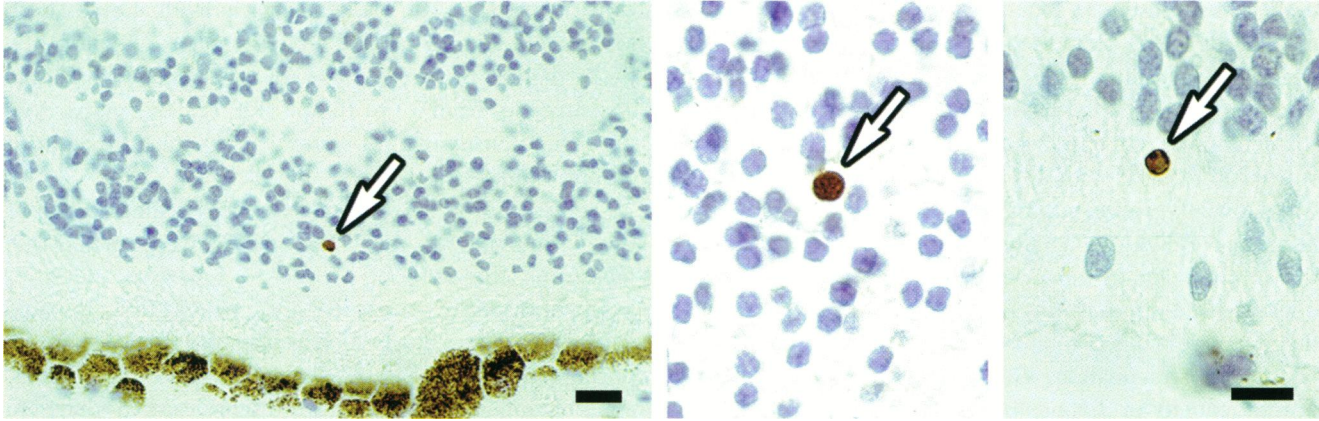


FIGURE 8

Retinas with diabetic retinopathy labeled with TUNEL technique for identifying dying cells (possibly by apoptosis). Left, Radial section from subject D6 (Table I). One positively stained cell is seen in outer nuclear layer (arrow, brown reaction product). Bar = 20  $\mu\text{m}$ . Middle, Higher magnification of positive cell in outer nuclear layer of another diabetic retina (arrow) (subject D1, Table I). Right, Positive ectopic nucleus located sclerad to external limiting membrane (arrow) (subject D1, Table I). Bar = 10  $\mu\text{m}$  (same magnification as middle panel).

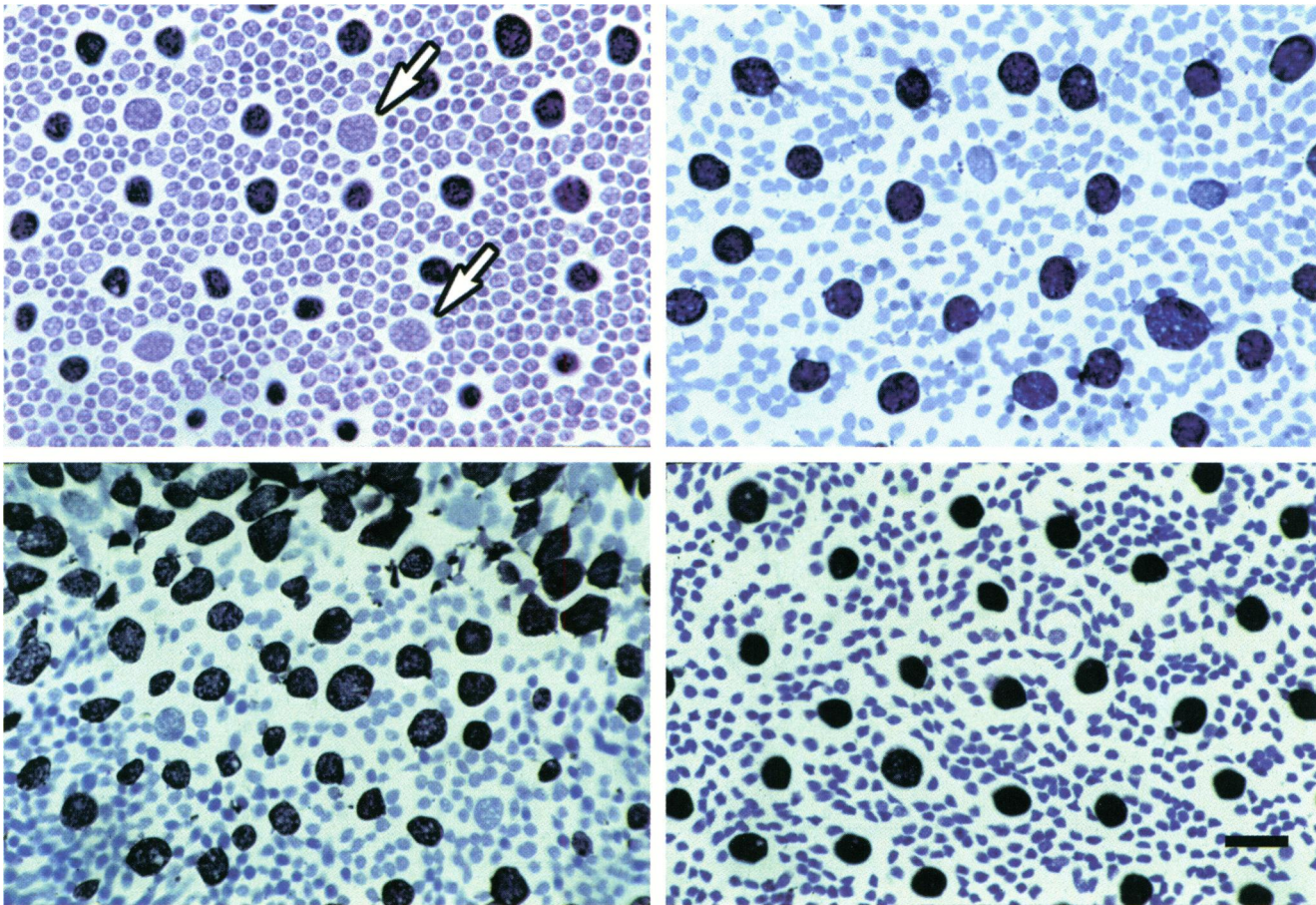


FIGURE 9

Tangential sections at level of photoreceptor inner segments located 10 to 20 arc degrees from fovea. Enzyme histochemical reaction for carbonic anhydrase (CA) produces a black reaction product, which labels dominant, L/M-cones. Upper left, Section from 68-year-old woman with no known history of ocular disease (control C5, Table I). Roughly 9% of cones are blue-sensitive (arrows, CA-negative). Upper right, Section from similar area in another 68-year-old woman with proliferative diabetic retinopathy treated with laser photocoagulation (D5, Table I). Fewer CA-negative cones are present. There are also fewer rods than in control section. Lower left, Another section from same subject as in upper right showing focal area with marked reduction in rods. L/M-cone density is essentially unchanged. Lower right, Section from another diabetic retina (D6, Table I). Note lack of S-cones, decreased density of rods, and poorly defined cone sheaths (toluidine blue counterstain; Bar = 10  $\mu\text{m}$ ).

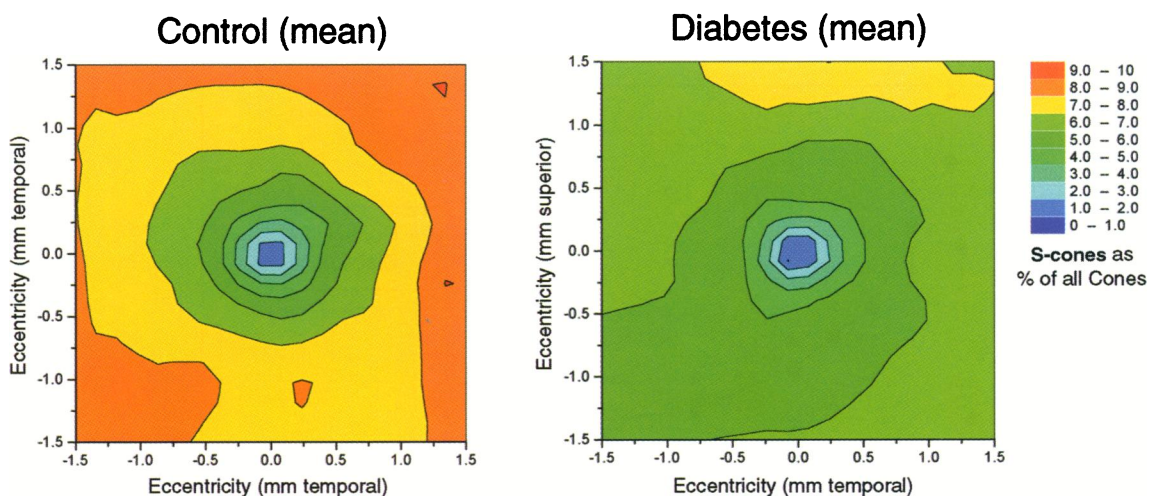


FIGURE 10

Topographic two-dimensional plots showing percentage of S-cones (carbonic anhydrase–negative) versus retinal eccentricity for maculae of all control eyes (left) and all diabetic eyes (right). There is a generalized reduction of percentage of S-cones in all directions for diabetic retinas.

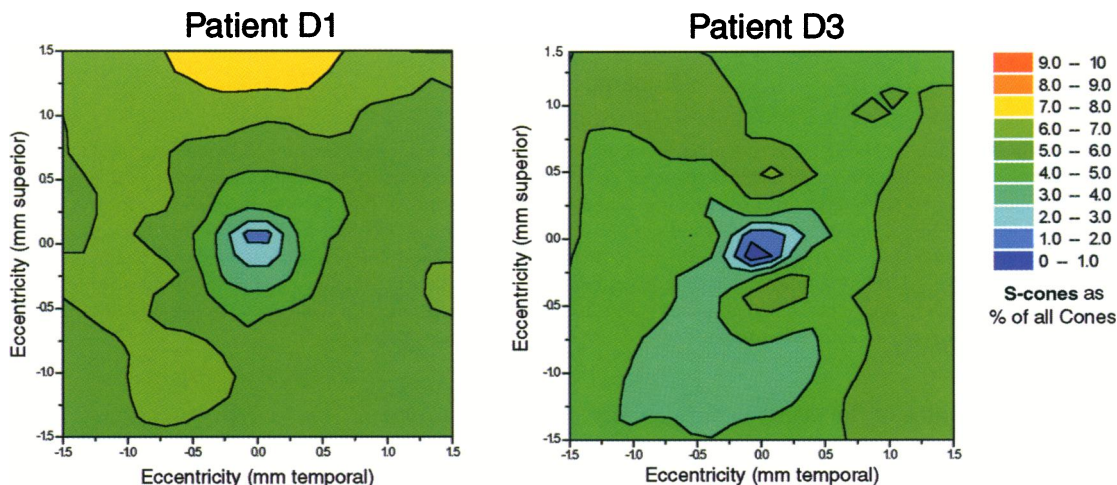


FIGURE 11

Plots similar to Figure 10 for 2 individual diabetic retinas (subjects D1 and D3, Table I). Distribution pattern is somewhat more irregular than means plotted in Figure 10.

small sample size, it was not possible to correlate S-cone loss and severity of disease. Simple inspection of the post-mortem retinas with the dissecting microscope is not a substitute for detailed history, because diabetic retinopathy can become inactive after several years—leaving little evidence of damage at this level.

Given the limited ocular histories for some of the subjects and especially for the controls, it is important to consider the other retinal diseases that might be common enough to act as confounding variables. The only entity that fits this category is glaucoma. Although macular degeneration is quite common among this age-group, even mild forms of the disease are easily identified on inspection of the posterior poles with the dissecting microscope. No such eyes were included in this study. By

contrast, glaucoma is often not evident in gross specimens. Moderate cupping of the optic nerve can be obscured by postmortem changes and fixation. Glaucoma is also a concern because it may<sup>82-84</sup> (or may not)<sup>85,86</sup> be more prevalent in patients with diabetes mellitus. Furthermore, glaucoma is now known to affect the photoreceptors in the outer retina.<sup>81</sup> Even so, Klein and colleagues<sup>83</sup> found that the difference in the prevalence of glaucoma between patients with older-onset diabetes and those without diabetes was only 2.2% (4.2% versus 2%, respectively), so it is unlikely to be a major factor in such a limited sample as ours. More important, most of the outer retinal damage in glaucoma seems to be concentrated in the L/M-cones,<sup>81</sup> whereas the S-cones were selectively lost in our diabetic eyes.

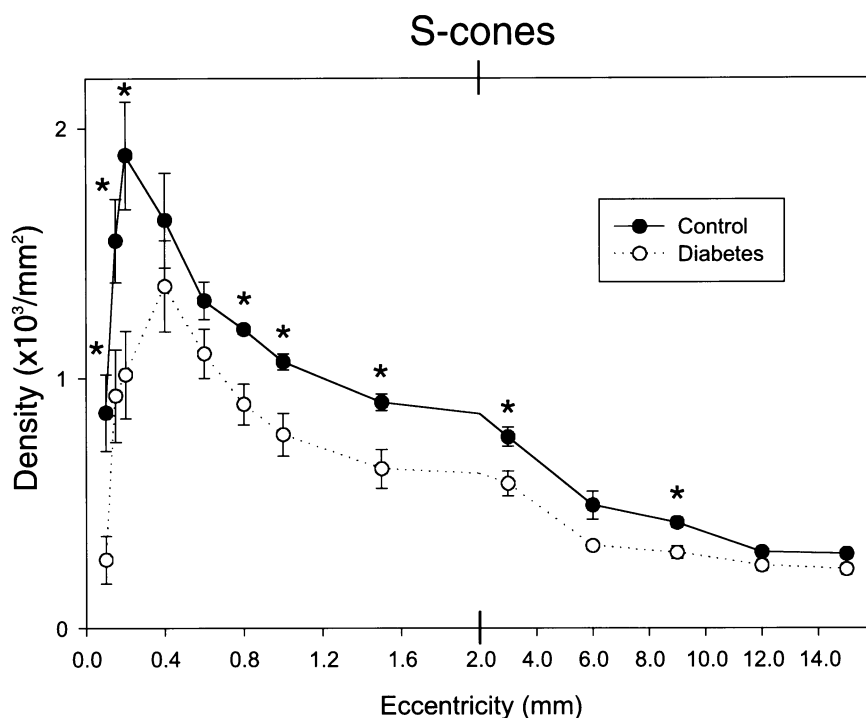


FIGURE 12

Density of S-cones as function of retinal eccentricity  $\pm$  standard error of mean (SEM). An analysis of variance (ANOVA) was used to examine whether S-cone density at various eccentricities differed between diabetic and control subjects. Eccentricity, a repeated measures variable, was evaluated with Huynh-Feldt adjustments to degrees of freedom to correct for correlated repeated measures. A Type IV sum-of-squares error term was used because of missing data at some eccentricities. S-cone densities differed significantly with eccentricity ( $F(1,8.92) = 32.05, P < .01$ ). There was no overall difference in densities between groups ( $F(1,2) = 10.89, P = .082$ ). However, there was a significant difference between groups in S-cone density with eccentricity ( $F(1,8.92) = 3.89, P < .005$ ). Asterisks (\*) indicate that differences in means are significant ( $< .05$ ) by independent samples Student's *t*-Test, assuming unequal variances and evaluated using a one-tailed probability distribution (due to constraint that diabetic L/M-cone densities cannot exceed control values). Diabetic retinas show significantly lower mean S-cone density at most eccentricities.

TUNEL labeling of some of the nuclei in our patients with diabetes was consistent with cell death in the inner nuclear as well as the outer nuclear layers in diabetic retinopathy. In such a chronic disease, which can last for years or decades, it is expected that even if cell death were common, only rare cells would be TUNEL-positive. This is because in cells undergoing death by apoptosis, there is only a relatively brief time interval during which the nuclei are TUNEL-positive—perhaps as short 1 to 3 hours in normally cycling cells of the intestine, epidermis, lymphoid tissue, and so on,<sup>75</sup> and 8 to 11 hours for ganglion cells in axotomized rats.<sup>77</sup> Finally, TUNEL labeling alone, although consistent with programmed cell death (apoptosis), does not rule out death by necrosis.<sup>78</sup> Nevertheless, TUNEL staining in our diabetic retinas and absence of such findings in control retinas suggests that retinal cell death is occurring in diabetic retinopathy.

Although diabetic retinopathy is sometimes thought of as an inner retinal vasculopathy, loss of photoreceptors indicates damage to the outer retina as well. Outer retinal injury might be predicted, considering the studies showing that choroidal vasculopathy is an important element in

this disease.<sup>89,90</sup>

Partial loss of S-cones could contribute to the color vision deficit in diabetic retinopathy. This does not rule out the possibility that factors in addition to photoreceptor death may be involved as well. Indeed, color vision deficits have been observed even in early diabetic retinopathy,<sup>41,60,72,91</sup> including patients with diabetes with angiographically normal retinas.<sup>92,93</sup> Unlike the findings of nearly total S-cone loss in human traumatic retinal detachment and experimental retinal detachment in monkeys, only a portion of the S-cones was lost. Therefore, the contribution of other prereceptor or postreceptor mechanisms cannot be ruled out.

#### L/M-CONE INJURY IN GLAUCOMA

(The next section briefly summarizes work previously done by the author and his associates. The full paper has been published.<sup>81</sup> It is presented here as background for the sections that follow.)

For the purposes of this thesis, the term "glaucoma" is used to mean moderate and low-pressure chronic

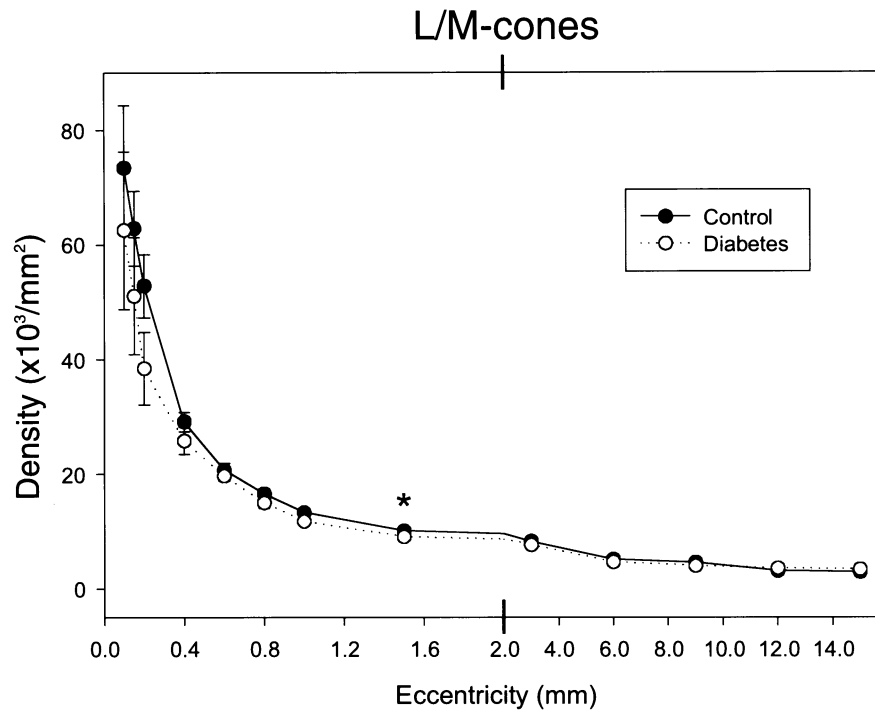


FIGURE 13

Density of L/M-cones as function of retinal eccentricity  $\pm$  SEM. Data were analyzed using same ANOVA design used for analyzing S-cones. Although densities change significantly with eccentricity ( $F(1,2.54) = 109.05, P < .001$ ), there is no difference between groups ( $F(1,10) = 1.95, P > .19$ ), nor do groups differ significantly by eccentricity ( $F(1,2.54) = 0.41, P > .71$ ). Student's *t*-Tests performed as for S-cones density data (Fig 12), was significant (\*) for only one of 13 tests.

glaucoma. Primary open-angle glaucoma (POAG) is the most common form of this condition.

#### Introduction

Glaucoma is an apparent exception to Köllner's rule of acquired color vision loss. Visual loss in this disease occurs because the retinal ganglion cells die, probably by apoptosis.<sup>94,95</sup> Traditionally, elevated intraocular pressure (IOP) is thought to gradually and irreversibly damage the ganglion cell axons in the optic nerve and thereby cause retrograde degeneration of their cell bodies. The mechanism by which elevated pressure causes death of the optic nerve fibers has been assumed to be direct; either by reducing the blood flow to the nerve<sup>96,97</sup> or by causing an outward deformation of the lamina cribrosa with the subsequent interruption in axoplasmic flow.<sup>98</sup>

A peculiar aspect of the vision loss in patients with glaucoma is the type of color vision deficit observed. Given the putative involvement of the optic nerve in the etiology of glaucoma, it would be expected that color vision loss would be along the red-green axis. Patients with glaucoma, by contrast, confuse colors along the blue-yellow axis.<sup>99-103</sup> This is often explained by assuming that those axons responsible for conveying blue-yellow opponent data are more susceptible to damage than those transmitting

red-green information. However, such an explanation remains controversial. Quigley and coworkers have shown anatomic<sup>104</sup> and biochemical<sup>105</sup> differences between glaucomatous and other forms of optic nerve damage, with the former affecting mostly the region of the lamina cribrosa. Glaucomatous cupping may be associated with deformation of the axons as they pass through the lamina.<sup>98,106,107</sup> Quigley and associates have also clearly demonstrated that there are 2 aspects to axonal loss.<sup>108,109</sup> Those axons passing over the superior and inferior edges of the optic nerve are lost earlier in the disease process than the nasal and temporal fibers, which might explain the paracentral and arcuate defects seen on visual field testing. There may also be a generalized loss of axons with the larger-diameter fibers being lost earlier than the smaller fibers.

However, such an explanation remains controversial. While the axons supplying blue-yellow information may be somewhat larger than the red-green axons.<sup>110</sup> The largest ganglion cells are mostly the phasic axons,<sup>111</sup> which respond vigorously to luminance contrast and to high temporal frequencies and are relatively insensitive to purely chromatic differences.<sup>112</sup> The tonic axons are devoted to blue-yellow or to red-green opponent information<sup>112</sup> and are smaller in diameter compared to the phasic axons.<sup>110</sup>

Could this blue-yellow color deficit be based on

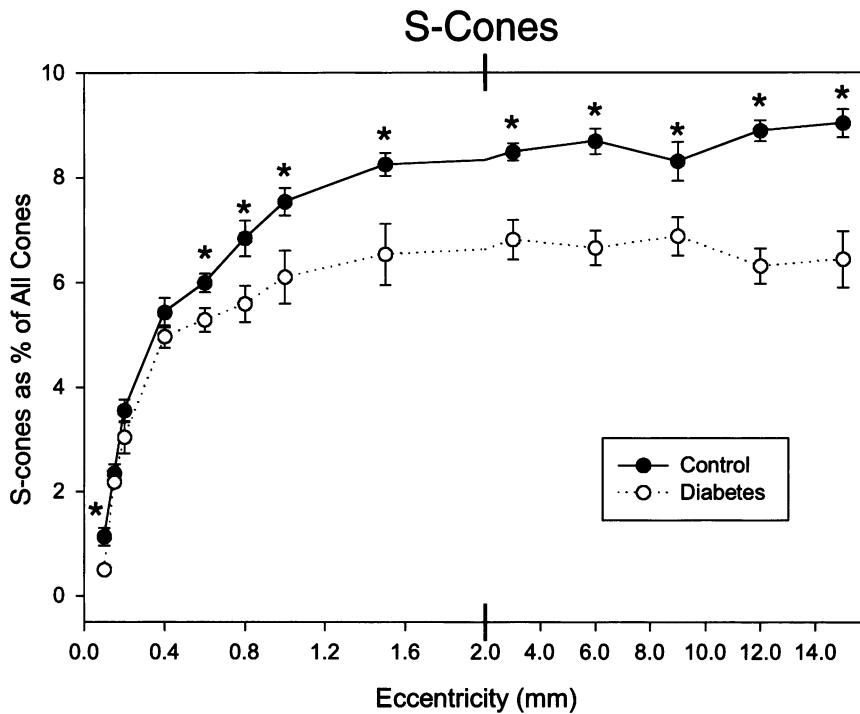


FIGURE 14

Percentage of cones that are blue-sensitive as function of retinal eccentricity (means for all directions) extending to 15 mm  $\pm$  SEM. A greater number of missing cells from joint occurrence of S- and L/M-cone density data sets precluded performing an ANOVA. Independent groups' *t*-tests were performed as for density data in Figs 12 and 13, however a two-tailed test was used, since relative percentage of S-cones is not constrained and could increase if there were a decrease in L/M-cones. In patients with diabetes, most eccentricities have a significantly lower mean percentage of S-cones compared to controls (\*). Note scale change at 2 mm eccentricity.

photoreceptor damage as was found in retinal detachment<sup>53</sup> and diabetes?<sup>113</sup> Histopathologic evidence for photoreceptor injury in high-pressure glaucoma is unequivocal. Anderson and coworkers<sup>114</sup> observed focal dropout of photoreceptors in the owl monkey. Ultrastructural defects suggestive of programmed cell death (apoptosis) were noted by Büchi and colleagues<sup>115,116</sup> in nuclei of the outer retina in a rat model of pressure-induced ischemia. In human eyes with secondary angle-closure glaucoma, Panda and Jonas<sup>117</sup> counted significantly fewer photoreceptors compared to normal subjects. Janssen and associates<sup>118</sup> found fewer photoreceptors compared to controls as well as pyknotic nuclei in the outer nuclear layer in 2 human eyes with secondary, painful glaucoma (IOPs >40 mm Hg).

By contrast, anatomic evidence for outer retinal injury in chronic (moderate-pressure) glaucoma has been lacking. Loss of photoreceptors was not found in human eyes with primary open-angle glaucoma in a study by Kendell and coworkers.<sup>119</sup> Nor did Wagnanski and colleagues<sup>120</sup> observe cone loss with experimental glaucoma in cynomolgus monkey.

Although morphologic indications of photoreceptor deficit had been lacking, investigations using the electroretinogram (ERG) suggest something else. The ERG is generated mostly by the photoreceptors and the bipolar

cells and is not altered by optic nerve transection; therefore, it should not be affected if glaucomatous damage is limited to the optic nerve and inner retina. Traditional thinking suggested that this was the case, yet recent work, using careful quantification and proper selection of controls, now provides strong evidence of outer retinal effects in humans.<sup>121-125</sup> Furthermore, Weiner and associates<sup>126</sup> found that foveal cone ERG amplitude was subnormal in a significant proportion of glaucomatous eyes. On the other hand, outer retinal ERG changes were not seen in a monkey model of experimental glaucoma.<sup>127</sup>

Reasoning that the outer retina is, indeed, involved in glaucoma but that the morphologic changes were too subtle to see on traditional radially cut, paraffin-embedded retinas (ie, cut perpendicular to the plane of the retina), a study was performed in which the retinas were embedded in glycol methacrylate plastic, which permitted making thinner sections than was possible with paraffin. In addition, the sections were cut tangentially to the globe (parallel to the plane of the retina), so that greater numbers of photoreceptors could be examined per microscopic field.

#### Methods

In this study, the outer retinas from 128 human eyes with a diagnosis of chronic glaucoma (presumably POAG in

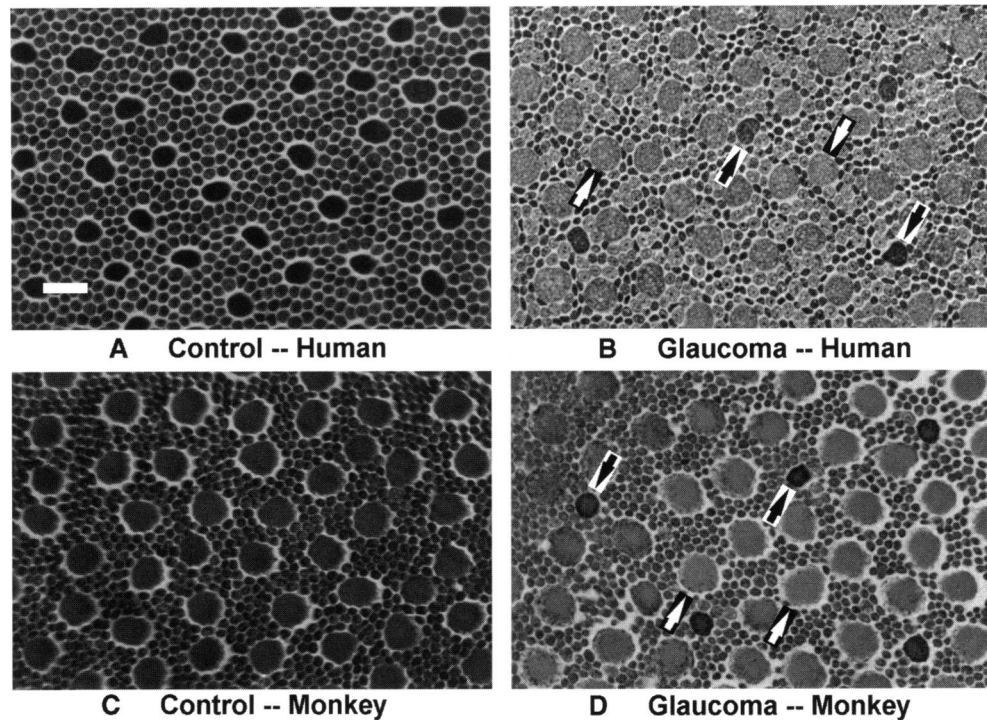


FIGURE 15

Inner segments tangential sections. A, Normal human retina. B, Retina from same area of another human with primary open-angle glaucoma (POAG). C, Normal (control) rhesus monkey retina. D, Retina from same region of animal's fellow eye with experimentally induced glaucoma. In human and monkey controls, subtypes of cones (red-, green-, and blue-light sensitive) are indistinguishable. However, for both human and monkey glaucoma, 2 distinct cone populations are apparent. Dominant cone population (probably L/M-cones) is swollen (white arrows) compared to a minority population, possibly S-cones (black arrows) (toluidine blue; bar = 10  $\mu$ m).

most cases) and 90 control eyes were examined histologically by 3 masked observers for photoreceptor swelling and loss. Retinas from 9 rhesus monkeys with glaucoma induced experimentally by laser trabecular destruction were compared to retinas from 7 fellow (control) eyes. The mean pressure elevations in the eyes with laser trabecular destruction ranged from 26.6 to 53.6 mm Hg with durations varying from 7 to 33 weeks.

### Results

Swelling of the red- and green-sensitive cones was observed in a significantly greater proportion of human eyes with presumed POAG compared to the control eyes (Fig 15). Patchy loss of L/M-cones and rods was also found in some of the glaucomatous retinas (Fig 16). In a subset of the human eyes with end-stage disease, cone swelling was a variable finding. Although no photoreceptor loss was found in the 9 monkey eyes with experimental glaucoma, 8 had swelling of their L/M-cones that was remarkably similar to that seen in the human eyes (Fig 15). Swelling was not present in any of the control monkey eyes.

### Conclusions

This study shows that glaucoma is associated with anatomic

changes to the photoreceptors. As such, it may be that glaucoma is actually consistent with Köllner's rule in the sense that it is, at least in part, a retinal degenerative process. The situation is distinct from earlier work with retinal detachment and diabetic retinopathy where selective loss of the S-cones was found.<sup>53,128</sup> The human and monkey eyes with glaucoma showed mostly swelling and loss of the L- and M-cones. However, an apparent shrinkage of the S-cones was also seen in some of the monkey eyes (Figs 15C and 15D).

Although it is only possible to speculate about function based on morphology, recent careful analysis of the blue-yellow deficit in glaucoma reveals that unlike other retinal disorders, in which there is relatively more selective suppression of the S-mechanism,<sup>37,59,129</sup> in glaucoma there is significant decrease in the sensitivity of the L- and M-systems as well as the S-pathway.<sup>130</sup> Likewise, a behavioral study in an experimental model of POAG in monkey has shown that early glaucomatous changes affect mostly the S-pathways but that the L- and M-systems are involved in more advanced disease.<sup>131</sup> Perhaps changes in the L- and M-cones were found to be so common because these subjects had advanced disease or because the L/M-cone swelling is easier to detect than more subtle biochemical changes that might be occurring in the S-cones.

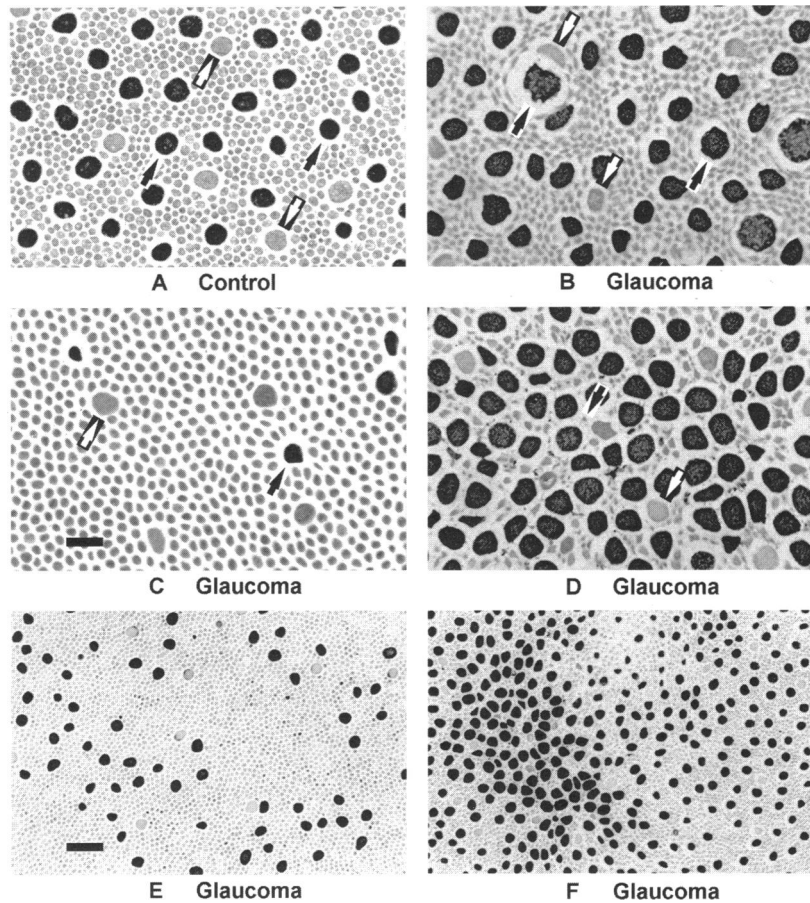


FIGURE 16

Human inner segments, reacted for CA—tangential sections. A, Normal human retina shows positive staining for CA in 91% of cones (black arrows), but rods and about 9% of cones (white arrows) are negative. These CA-negative cones are the S-cones (blue-sensitive).<sup>26</sup> B, Same region from eye with POAG. Swelling of inner segments is confined to CA-positive cones (L/M-cones, black arrows), while S-cones (white arrows) are not obviously enlarged. C, Another subject with POAG from same region as in A and B. Marked loss of CA-positive cones (black arrow) is present. However, CA-negative S-cones (white arrow) have normal distribution within this frame. D, Another glaucomatous eye showing focal rod (black arrow) dropout. There is an increase in density of cones, probably a result of sliding together of adjacent cones to take up space left by missing rods. Note that both CA-positive and CA-negative (white arrow) cones remain. E and F, Lower magnifications of retinas shown in C and D, respectively. Patchy nature of photoreceptor loss is evident. Even though a proportionately greater loss of L/M-cones compared to S-cones is present in E, all cone types are missing from large central area (toluidine blue counterstain; bars = 10  $\mu\text{m}$  [A through D] and 25 $\mu\text{m}$  [E and F]). Contrast adjusted digitally to optimize conversion from color to grayscale.

Because of the spectral opponency aspect of color vision, decreased sensitivity (or actual loss) of either the S-cones alone or a process that equally affects both the L- and M-cones could result in blue-yellow confusion.

Indeed, all 3 cone types could be injured and the result would still be blue-yellow confusion, as long as the L- and M-cones respond equally and the S-cones are affected to a relatively greater or lesser extent. Equivalent response in L- and M-cones is not an unreasonable scenario considering the 96% identity of the amino acid sequences<sup>33</sup> of the L- and M-cone opsins, as well as many other biochemical similarities between the L- and M-cones, such as the carbonic anhydrase<sup>26</sup> and calbindin<sup>132</sup> distributions, and the immunochemical similarity of S-antigen isoforms,<sup>36</sup> and so on.<sup>133</sup> By contrast, the S-cones

share only a 43% identity in the amino acid opsin sequences compared to L- or M-cones. S-cones even differ morphologically from the longer-wavelength cones.<sup>25</sup>

#### **ANTEROGRADE HYPOTHESIS OF GANGLION CELL DEATH IN GLAUCOMA**

##### **BACKGROUND AND HYPOTHESIS**

The finding of photoreceptor injury in both human glaucoma and experimental glaucoma in a monkey model raises the intriguing possibility that damage to the outer retina may contribute in some way to the disease process. Of course, the other two possibilities are that the photoreceptors are



simply responding to ganglion cell changes or that this is an independent site of pathologic change, unrelated to ganglion cell death. In the following sections, arguments will be put forward in support of this first idea—that photoreceptor injury may contribute to ganglion cell death. Experiments designed to test the predictions of this hypothesis will then be presented.

#### *Distribution of Outer Retinal Changes in Glaucoma*

If there is a relationship between photoreceptor injury and ganglion cell death, (ie, if the two phenomena do not represent two separate sites of damage), one would expect that the average distribution of swollen cones in moderate (not end-stage) disease should be predominantly in the arcuate region—similar to the average distribution of ganglion cell loss known to occur in moderately advanced glaucoma. Although the study cited above did not address this issue (only a single location in the arcuate region was examined), some recent investigations do.

Nickells and colleagues<sup>134</sup> reasoned that if the cones are injured, they would produce opsin at a slower rate. To avoid problems introduced by protein turnover, they decided to get a more accurate picture of gene expression by looking at opsin mRNA production. cDNAs of about 200 (bp) long and specific for L/M-cone, S-cone, and rod opsins were generated by polymerase chain reaction. These cDNAs were subcloned into plasmids and used to generate antisense probes for in situ hybridization and RNase protection analyses. Experimental glaucoma was produced by laser trabecular destruction in monkeys as described above. In the arcuate region, there was marked reduction of mRNA seen by in situ hybridization for the L- and M- as well as the S-cones, but not for the rods.

In a related experiment by the same authors,<sup>134</sup> samples of retina were removed from the macula, arcuate region, and peripheral retina and processed for RNase protection assay—a method that quantifies mRNA levels. By calculating ratios of rod opsin (rhodopsin) to L/M-opsin in these 3 locations, the investigators showed that the arcuate region was most affected. (This technique is not sensitive enough to detect the S-cones because they are so few in number.)

In yet another line of investigation, Ver Hoeve and coworkers<sup>135</sup> have now demonstrated L/M-cone injury in human glaucoma using the multifocal electroretinogram (mERG). mERG has been explored for its utility in glaucoma by others. However, the emphasis has been on those components of the mERG that are most likely to measure ganglion cell function.<sup>136-139</sup> Vaegan and Buckland,<sup>140</sup> on the other hand, did find that the first kernel of the mERG was affected in glaucoma—a probable measure of outer retinal function.

Dr Ver Hoeve took another approach. He deliberate-

ly selected a component of the ERG that most closely corresponds to L/M-cone function—namely, the photopic latency (time from stimulus to the trough of the a-wave). He and his associates found that 8 of 9 patients with clinically diagnosed glaucomatous field loss showed significant increases in the latency of the early waves in a paracentral pattern extending from the disk. Although these areas of increased mERG latency did not necessarily coincide with visual field losses, when averaged together, the distribution of the increased latencies was similar to the average visual field losses seen in early and moderate glaucoma.<sup>141</sup>

#### *Could the Photoreceptor Swelling be Simply a Response to Dying Ganglion Cells?*

This question was partially addressed in the paper discussed in the preceding section. Tangential sections at the level of the ganglion cells were examined in all 128 human eyes with a diagnosis of glaucoma. Twenty of these had severe (>90%) loss of the ganglion cells (ie, end-stage disease). Five of the 20 (25%) had marked swelling of the L/M-cones. However, 7 of the eyes with severe ganglion cell dropout (35%) had no sign of photoreceptor swelling. If the photoreceptor swelling is a response to dying ganglion cells, then one would expect to see no photoreceptor swelling in eyes with end-stage disease, (ie, those retinas with no or few surviving ganglion cells). However, when the subset of eyes with more than 90% ganglion cell loss was examined, some eyes had marked cone swelling and some had no detectable swelling (the remainder had intermediate or questionable swelling). In other words, the photoreceptor changes could not be the result of degenerating ganglion cells, since there were almost no ganglion cells remaining in this subset of subjects; yet there is no consistent pattern of photoreceptor swelling. Indeed, photoreceptor swelling may well be a transient response to decreased choroidal blood flow—resolving once the blood flow has been restored to normal levels, such as by adequate IOP management.

In another study, in situ hybridization was done using the same 3 probes for the photoreceptor opsins as described above, but with a monkey that had optic nerve transection posterior to the insertion of the central retinal artery and vein (unpublished data). Five and one-half weeks after transection, the eyes were enucleated, fixed, and underwent in situ hybridization. There was no significant difference in either the rod, S-cone, or L/M-cone opsin staining between the eye with optic nerve transection and the fellow control eye. Thus showing that, with a known optic neuropathy, and under these conditions, the photoreceptors do not seem to be affected by the dying ganglion cells.

#### *Choroidal Blood Flow in Glaucoma*

Swelling of the cones, as with other neurons, may indicate

ischemic injury, which could arise from a decrease in choroidal circulation. Only a moderate increase in the IOP in cats leads to a reduction in choroidal blood flow and a precipitous fall in oxygen saturation at the vortex veins.<sup>142,143</sup> Consistent with this, functional changes specific to the outer retina—decreased electroretinographic c-wave and the dark adapted standing potential—have been shown to be reduced in cat and monkey with experimentally induced IOP elevations as low as 15 to 20 mm Hg above baseline.<sup>144</sup> In humans with POAG, several studies using Doppler ultrasonography have shown that blood flow is significantly decreased in the ophthalmic artery, most of whose circulation supplies the choroid.<sup>145-150</sup> Finally, histopathologic evidence suggests that there is loss of the innermost choroidal vessels in POAG.<sup>151</sup>

Although choroidal circulation is probably decreased in glaucoma, any hypothesis involving a role for the outer retina in ganglion cell death needs to account for the arcuate distribution of injury known to occur in early and moderate glaucoma. As noted above, the photoreceptor changes seem to follow this pattern, but what about the choroidal blood flow?

Choroidal blood flow is difficult to measure with great precision because of its location behind the retinal pigment epithelium and because of the overlying retinal vessels. Nevertheless, some useful information has been gleaned from studies of the regional variations in choroidal choriocapillary anatomy, experimental occlusion of the posterior ciliary artery in monkeys, and from investigations into the early filling phase of the fluorescein angiogram.

Traditional histopathologic studies of the choriocapillaris and choroid are limited because they are only able to look at small regions. This changed with the introduction of vascular casting techniques. Yoneya and Tso<sup>152</sup> employed corrosion vascular casts and scanning electron microscopy to examine the angioarchitecture of large areas of the human choroid in 9 normal autopsy eyes. They concluded that there were 3 distinctive patterns to the choriocapillaris depending on eccentricity from the fovea. They observed a lobular arrangement of the vessels in the posterior pole, giving way to a spindle pattern in the equatorial region and a ladder pattern in the periphery. Such variations have been confirmed by Fryczkowski and colleagues<sup>153</sup> who divided the circulatory patterns into 5 regions: submacular, posterior pole, equatorial, peripheral, and peripapillary. Interestingly, they noted that this “submacular” region did not show a lobular pattern. Instead, they found a freely interconnected monolayer of vessels. They also described abundant anastomotic connections between the submacular choroidal vessels.

Precisely how these regions relate to each other in terms of flow rates and anastomotic connections is not fully understood in the normal eye, much less in a dis-

eased one. However, Hayreh and Baines<sup>154,155</sup> provided some insight into these anatomic relationships with their study of the effects of occlusion of the posterior ciliary artery in 85 monkey eyes. The resultant lesions (acute white patches and subsequent discoloration of the fundus) showed a remarkable pattern. Although each animal had a distinctive arrangement of defects, overall there was a tendency for the defects to involve the midperipheral area (including the arcuate region involved in glaucoma) with relative sparing of the macula and far peripheral retina. Interestingly, many of the lesions respected the horizontal meridian. Consistent with this is an earlier study of microsphere occlusion in the choriocapillaris of rhesus monkeys by Stern and Ernest.<sup>156</sup> They found high concentrations of microspheres in the macula, which they interpreted as resulting from a greater blood supply from the short posterior ciliary arteries. Hayreh<sup>157</sup> has also described watershed zones in the choroidal circulation that are visible in early-phase fluorescein angiograms. As with the occlusion studies, these zones often respect the horizontal meridian.

Given these observations of variations in choroidal anatomy and blood flow, it seems reasonable, considering that choroidal blood flow is reduced in glaucoma, that this reduction would not necessarily be equal in all areas. Not many data are available to support this idea, although Vaegan and coworkers<sup>158</sup> have found delayed choroidal filling across the posterior poles of human glaucomatous eyes—confirming work done in 1970 by Rosen and Boyd.<sup>159</sup>

#### *Anterograde Hypothesis of Ganglion Cell Death in Glaucoma*

If the swelling of the L/M-cones is not simply a response to ganglion cell death, then why does the distribution of the swelling seem to mimic that of ganglion cell loss? It would be a rather unusual coincidence if the swelling represented a completely independent site of injury, which happens to correspond so well geometrically to the ganglion cell loss. A simpler explanation might be that the photoreceptors are involved in some way in the process of ganglion cell destruction.

Ganglion cells are known to survive in the absence of photoreceptors in such conditions as retinal laser photocoagulation,<sup>160,161</sup> retinitis pigmentosa,<sup>162</sup> and the RCS (Royal College of Surgeons) rat.<sup>163</sup> Thus, cell death due to a lack of trophic factors seems unlikely. However, ganglion cells are known to die by apoptosis in glaucoma,<sup>94,95</sup> and they contain N-methyl-D-aspartate (NMDA) receptors,<sup>164,165</sup> which, when acutely over-stimulated by glutamate, can lead to programmed cell death.<sup>166</sup> Elevated vitreous levels of glutamate have been found in POAG,<sup>167</sup> and it has recently been shown that chronically elevated levels of glutamate can trigger ganglion cell death as

TABLE II: COMPARISON OF RETROGRADE AND ANTEROGRADE HYPOTHESES

RETROGRADE	ANTEROGRADE
<ul style="list-style-type: none"> <li>• Increased intraocular pressure</li> <li>• Decreased blood flow to ON and/or mechanical deformation of lamina cribrosa</li> <li>• Decreased axoplasmic flow</li> <li>• Ganglion cell death</li> </ul>	<ul style="list-style-type: none"> <li>• Increased intraocular pressure</li> <li>• Decreased choroidal blood flow</li> <li>• Ischemia of L/M-cones (swelling) (decreased opsin mRNA production)</li> <li>• Decreased glutamate re-uptake (increased extracellular glutamate)</li> <li>• Overexcitation of bipolar cells</li> <li>• Overexcitation of ganglion cells</li> <li>• Ganglion cell death</li> </ul>

well.<sup>165</sup> Since glutamate is the major excitatory neurotransmitter of the photoreceptors,<sup>169</sup> it seems plausible that in glaucoma, the ischemia that may result from lowered choroidal blood flow could cause a decreased reuptake of glutamate. This would lead to excess glutamate in the intracellular compartment, which might reach the ganglion cells directly (by diffusion) and overexcite them. Alternatively, the increased extracellular glutamate might have an indirect effect by first overstimulating the bipolar cells, which would then overexcite the ganglion cells.

This will be referred to as the “anterograde” hypothesis to distinguish it from the traditional “retrograde” hypothesis, whereby the ganglion cells are thought to die as a result of neurotrophin deprivation because of either ischemic or mechanical damage directly to the ganglion cell axons as they pass down the optic nerve. Table II compares the steps in these two hypotheses.

Before tests of the anterograde hypothesis are discussed, one additional question should be addressed. Namely, why would injury to the L/M-cones, which constitute only about 5% of the total photoreceptor population, have such a significant impact on the majority of the ganglion cell population in glaucoma? An answer may lie in the fact that the L/M-cones have a disproportionately large input into the ganglion cells. About 80% of the ganglion cells are the parvocellular type (P-cells, midget ganglion cells),<sup>170,171</sup> which connect exclusively to cones. Other types of ganglion cells also have connections to the cones. Furthermore, the L/M-cones represent 91% of the total number of cones. Therefore, if the L/M-cones are affected by a disease process (even if the other photoreceptor types are not), and this damage is transmitted downstream, a large fraction of the ganglion cells might be involved.

In the following section, experiments are described that were specifically designed to test the predictions of the anterograde hypothesis versus the traditional retrograde hypothesis.

#### TESTS OF THE ANTEROGRADE HYPOTHESIS

A key feature of this anterograde hypothesis is that it requires chronically injured photoreceptors. Ganglion cells

do not depend on upstream neurotrophic stimuli as evidenced by their survival in such conditions as retinal laser photocoagulation,<sup>160,161</sup> retinitis pigmentosa<sup>162</sup> and the RCS (Royal College of Surgeons) rat.<sup>163</sup> Therefore, if the photoreceptors were to be focally ablated prior to induction of experimental glaucoma, there might be a protective effect on the overlying ganglion cells, which would not be predicted by the traditional retrograde hypothesis (Fig 17).

The results of such an experiment are presented, in which the photoreceptors were focally removed using retinal laser photocoagulation prior to induction of experimental glaucoma in rhesus monkeys. Consistent with the anterograde hypothesis, a protective effect on the ganglion cells was observed. No protection was seen in a similar experiment in which the retinal laser was followed by transection of the optic nerve.

#### Materials and Methods

*Retinal Laser Photocoagulation Followed by Induction of Experimental Glaucoma.* All animal procedures adhered to the Association for Research in Vision and Ophthalmology (ARVO, Rockville, Maryland) statement on the use of animals in vision research.

Eight eyes of 4 rhesus monkeys underwent retinal laser photocoagulation. The laser spots using the argon green wavelength (514.5 nm, Coherent, Santa Clara, California) were applied to the region of the posterior pole that corresponds to early visual field loss in humans with glaucoma, (ie, 5 to 20 arc degrees eccentric to fixation). Various spot sizes were created from 100  $\mu\text{m}$  to 4,000  $\mu\text{m}$  (spots more than 1,000  $\mu\text{m}$  were made by applying confluent 200- $\mu\text{m}$  individual burns), with energies from 50 to 130 mW and exposure times from 0.1 to 0.5 second.

After about 1 month (enough time to permit the debris of photocoagulation to be cleared by the retina), argon laser trabecular destruction (ALTD) was performed in 1 eye of 3 animals.<sup>172-174</sup> Briefly, a Kaufman-Wallow single-mirror monkey gonio lens (Ocular Instruments, Inc, Bellevue, Washington)<sup>175</sup> was used to deliver the laser to the trabecular meshwork. During each treatment session, either 270° or 360° of the anterior (non-pigmented)

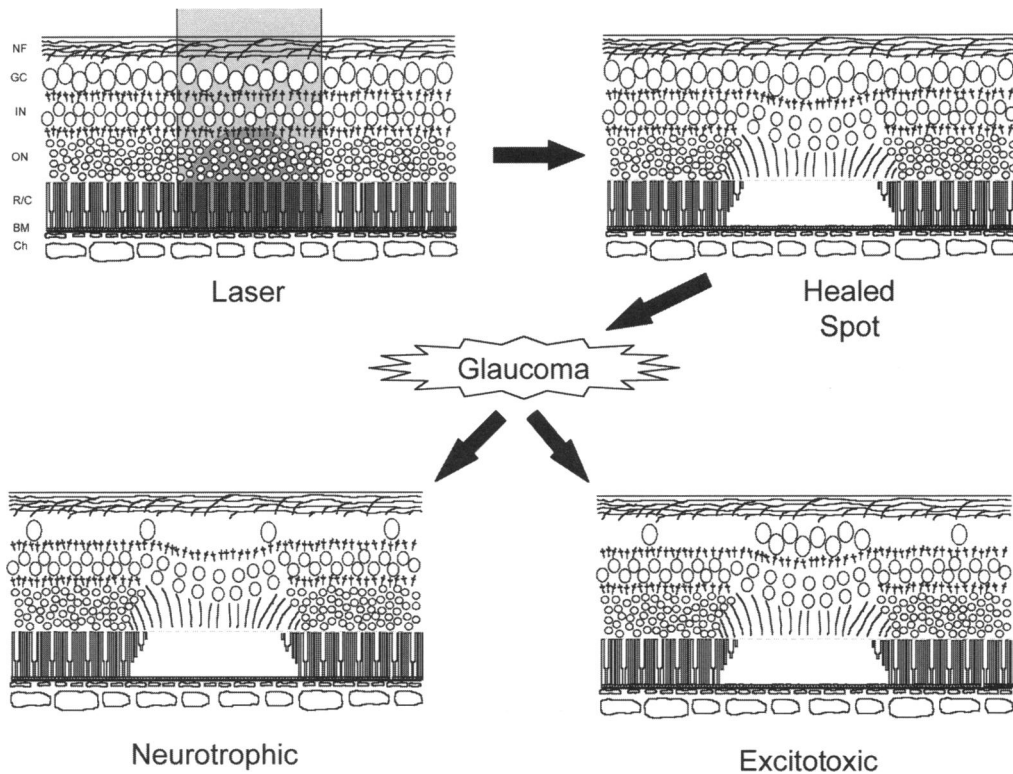


FIGURE 17

Design of experiment to discriminate between retrograde and anterograde hypotheses of ganglion cell death in chronic glaucoma. First, a retinal laser is applied (light gray), which is absorbed by pigment epithelium and converted to heat (dark gray) that kills photoreceptors (upper right). Experimental glaucoma is then produced by argon laser trabecular destruction. Two hypotheses predict different outcomes with respect to survival of subset of ganglion cells overlying healed laser spot (lower half). BM, basement membrane; Ch, choroid; GC, ganglion cell layer; IN, inner nuclear layer; NF, nerve fiber layer; ON, outer nuclear layer; R/C, rod/cone layer.

meshwork was photocoagulated with 514.5 nm of argon green laser using either 50- or 100- $\mu\text{m}$  spots of 1.0-Watt intensity and 0.5-second duration. Seventy-five to 200 such spots were applied per session. The IOP, which was measured twice weekly with a handheld digital tonometer (Tono-Pen XL; Mentor O & O, Nowell, Massachusetts), usually took 3 weeks to rise, and the elevation lasted variable lengths of time. (This device was found to underestimate the IOP at higher pressures in the cynomolgus monkey.<sup>176</sup> A similar study has not been done for the rhesus, although its eye, being intermediate in size between the human and the cynomolgus monkey, might be expected to have a smaller error than that found in the cynomolgus monkey.) Additional laser treatments were carried out as needed to maintain elevated pressures. Two sessions of ALT-D were administered to monkeys No. 1 and No. 3, and 4 sessions were used for monkey No. 2. In 1 animal (monkey No. 1), 1 drop of 0.5% timolol maleate (Timoptic, Merck & Co, Whitehouse Station, New Jersey) was applied to the cornea of the treated eye on 2 occasions to lower the IOP.

**Optic Nerve Transection.** To control for the possibility that retinal laser photocoagulation may promote retinal

ganglion cell (RGC) survival by mechanisms other than photoreceptor removal, the optic nerve was transected (instead of inducing experimental glaucoma) in 1 eye of 1 animal. As with the other monkeys, the fellow eye underwent retinal laser photocoagulation only. The optic nerve transection (ONT) was accomplished using the technique described by Gonnering and coworkers.<sup>177</sup> Briefly, a lateral orbitotomy was first performed. The optic nerve was then transected 6 to 8 mm behind the globe posterior to the entry of the retinal artery and vein. On recovery (approximately 1 week), a fluorescein angiogram with the animal receiving ketamine anesthesia was obtained to demonstrate patency of the retinal artery.

**Histologic Preparation.** The animals were euthanized, and the eyes were removed within 10 minutes and promptly chilled in 0.1 M sodium phosphate buffer (pH 7.4) at 4°C. Within 5 minutes, they eyes were removed from the buffer and cut coronally just anterior to the equator. The posterior pole was fixed in 4% paraformaldehyde at 4°C for 24 hours and then stored in 0.1 M sodium phosphate buffer (pH 7.4) at 4°C. Segments of retina containing individual laser spots were removed and embedded in glycol methacrylate, sectioned at a thickness of 1.9

*Acquired Color Vision Loss and a Possible Mechanism of Ganglion Cell Death in Glaucoma*

μm, and stained with thionin.

*Two-Dimensional Reconstructions.* Serial sections were cut through some of the retinal laser spots. For each histologic section, the nucleoli of cells in the ganglion cell layer that had the anatomic characteristics of RGCs (ie, large round nuclei, prominent nucleoli, abundant cytoplasm, and metachromatic thionin staining consistent with Nissl substance) were identified. The position of each nucleolus of cells meeting these criteria was measured with respect to a given point (either the midpoint of the smaller laser burns or the edge of the large, confluent burns) using a micrometer in the ocular of the microscope. Two-dimensional reconstructions of the laser spots were then plotted.

*Results*

*Retinal Laser Photocoagulation by Experimental Glaucoma.* Initially, the laser spots had a white appearance. After 3 weeks, they became darker with mottled pigmentation. The IOPs were elevated to variable degrees in the treated eyes (Table III).

In the RGC layers of the 3 monkeys treated with ALTD, increased densities of cells were seen over the large laser spots (Fig 18) relative to the surrounding retina. (The effect was not seen over the small laser spots.) These cells were located in a layer contiguous with the adjacent RGC layer. The inner plexiform layer and, in some cases, the inner nuclear layer were intact. Few cells were present in the inner plexiform layer. The cells in the ganglion cell layer over the laser spots had large round nuclei, prominent nucleoli, abundant cytoplasm, and metachromatic thionin staining that was consistent with Nissl substance. Only a few cells in this layer had spindle-shaped nuclei or contained cytoplasmic pigment granules (characteristic of activated glial cells, RPE cells, or macrophages), which were readily distinguishable from the putative RGCs.

To better illustrate the phenomenon, serial sections

were cut 1.9 μm thick through some of the laser spots. The locations of the putative RGC nucleoli were then measured and plotted on two-dimensional graphs. Figure 19 shows such a reconstruction comparing sections of retina from the same location of the temporal maculae in the left (control) and right (glaucomatous) eyes of monkey No. 1. Marked reduction in numbers of ganglion cells in the glaucomatous eye were seen everywhere except over the laser spot. Within the region where the photoreceptors had been ablated by previous retinal laser photocoagulation, the overlying putative RGCs are present in densities approaching that of the control eye (Fig 20).

At somewhat greater eccentricities than the spot shown in Fig 18, there are fewer RGCs normally present. Even so, the effect was still present, as shown in Fig 21. Unlike the more intense laser spot shown in Fig 18, the cells in the inner nuclear layer over these spots were present in apparently normal numbers; however, a downward stretching of this layer was seen. In addition, a few macrophages and/or activated RPE cells were present.

A similar effect was also found over the large, confluent laser spot in monkey No. 3 (Fig 22), where the average density of cells in the RGC layer over the lasered area in the glaucomatous eye was greater than the adjacent unlasered region (Fig 23). Unlike the more intense laser spot shown in Fig 18, the bipolar cells over these spots were present in normal numbers (not shown).

The mean densities as a function of foveal eccentricity for the sampled areas shown in Fig 23 were plotted in Fig 24. The densities were greater everywhere in the control eye (note the different vertical scales). Since the specimens were sampled from regions near the foveas (about 1 mm inferotemporal to the foveal centers, where ganglion cell density changes rapidly with eccentricity), these greater apparent densities in the control eye could be the result of the samples not being taken from corresponding areas. However, a generalized reduction in

TABLE III: INTRAOCULAR PRESSURES

MONKEY NO.	TREATMENT	DURATION (WK) <sup>o</sup>	MEAN IOP±SD (MM HG)	IOP RANGE (MM HG)†
1	ALTD	20	41±12	12-64
2	ALTD	22	45±15	16-69
3	ALTD	33	39±11	19-63
4	ONT	5.5	12±4	7-18

IOP, intraocular pressure; ALTD, argon laser trabecular destruction; ONT, optic nerve transection.

<sup>o</sup> Duration of IOP elevation for monkeys No. 1 through 3 and time between ONT and sacrifice for monkey No. 4.

† Range of pressures. IOP means do not include the IOPs during the intervals between the ALTD applications and the initial pressure rises for monkeys No. 1 through 3.

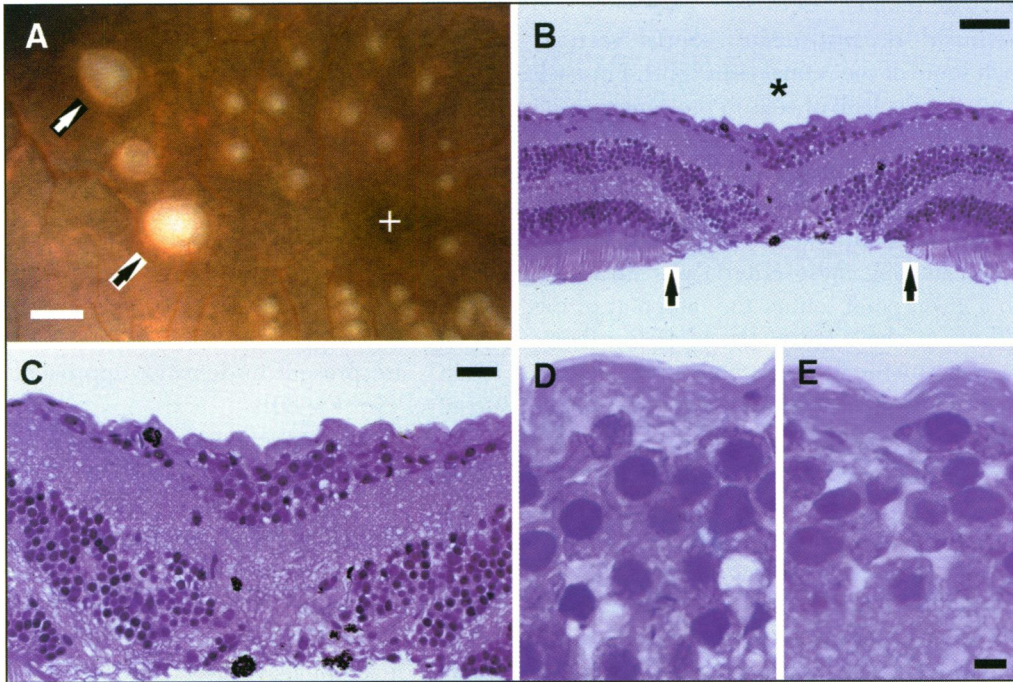


FIGURE 18

A, Fundus photograph immediately following retinal laser photocoagulation. After about 1 month, argon laser trabecular destruction was performed. Eye was enucleated after 142 days of elevated pressure. Fovea is indicated by plus sign (bar = 500  $\mu\text{m}$ ). B, Low magnification, and C, medium magnification of large laser spot (asterisk) shown by black arrow in part A. Ganglion cells are seen to survive primarily over laser spot. Arrows indicate border between viable and absent photoreceptors (toluidine blue; bars = 50  $\mu\text{m}$  [B] and 20  $\mu\text{m}$  [C]). D and E, High magnification of ganglion cell layer over laser spot (D) and in control eye (E). Note similar anatomy of cells (toluidine blue; bar = 5  $\mu\text{m}$ ). (D and E are same magnification). Histologic section of retinal laser spot indicated by white arrow in part A is shown in bottom half Fig 21.

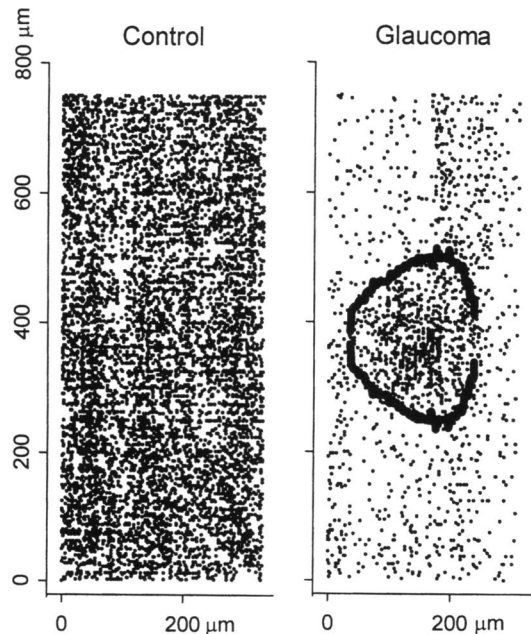
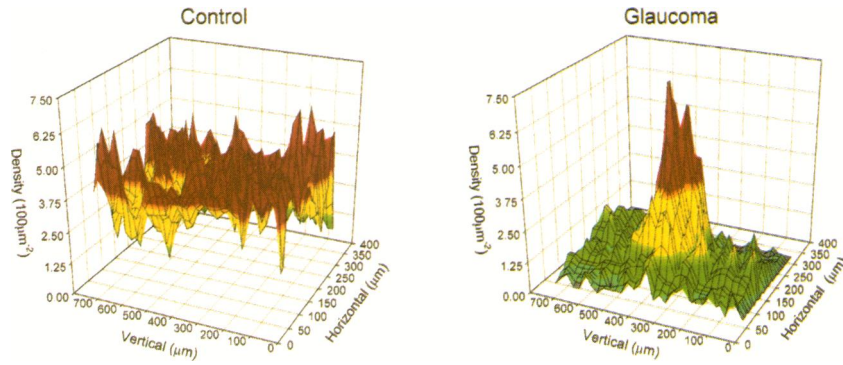


FIGURE 19

Two-dimensional reconstruction of ganglion cell layer from serial histologic sections. Each section is oriented vertically and was cut 1.9  $\mu\text{m}$  thick. Ordinate represents distance along a single section for any given position on abscissa. Points represent ganglion cell nucleoli. Control (left) shows area of retina in the control left eye centered 2 mm temporal to the fovea along the horizontal midline. There is no retinal laser spot in this region. Glaucoma (right) shows an area of retina from eye with experimental glaucoma corresponding to large laser spot indicated by black arrow in Fig 18A. This portion of retina has same temporal eccentricity as control. Thick black lines denote edge of laser spot in terms of surviving photoreceptors. Ordinates are oriented in superior (larger numbers)/inferior direction. Fovea is located to left of left plot and to right of right plot.

*Acquired Color Vision Loss and a Possible Mechanism of Ganglion Cell Death in Glaucoma*



**FIGURE 20**

Three-dimensional density plots of ganglion cells shown in Fig 19. Note that peak density over laser spot in eye with experimental glaucoma (red band) is similar to average density in control eye.

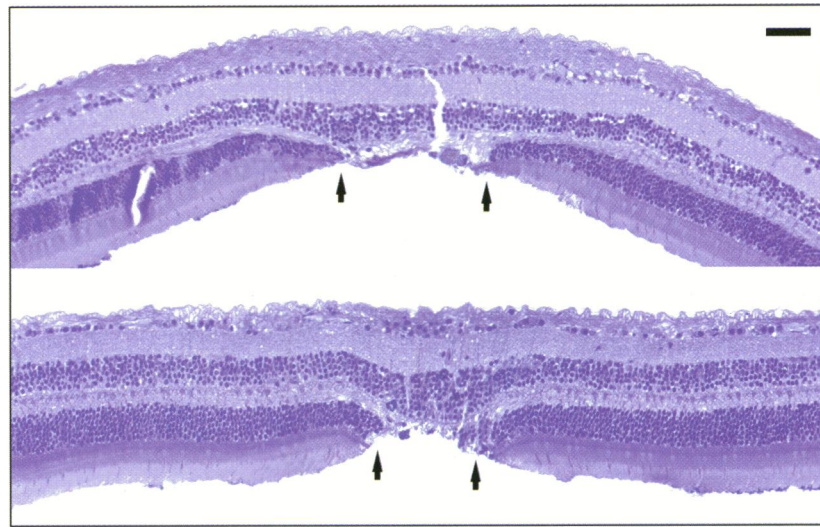


**FIGURE 21**

Comparison of 2 retinal laser spots of similar intensity and eccentricity in monkey No. 1. Arrows indicate border between viable and absent photoreceptors. Top, Control eye. Spot is 3 mm superior to foveal center. One or 2 layers of nuclei are present in ganglion cell layer. Density of cells in this layer over ablated photoreceptors is similar to surrounding, normal retina. Bottom, Glaucomatous eye. Spot is 3 mm superotemporal to foveal center (indicated by white arrow in Fig 18). As in A, 1 or 2 layers of nuclei are present in ganglion cell layer over ablated photoreceptors. However, density of cells in this layer is greatly reduced in surrounding, untreated retina (toluidine blue; bar = 50 µm).



**FIGURE 22**

Fundus photographs of both eyes for monkey No. 3 immediately following retinal laser photocoagulation. Note confluent patches in inferior maculae. Left, Experimental glaucoma was subsequently produced in right eye. White rectangles represent areas used for two-dimensional reconstruction (Fig 23). Right, Note that sampled area in control left eye is somewhat closer to fovea than treated right eye.

ganglion cell density in the eye with glaucoma could not be ruled out. The transition of densities across the edge of the laser spot was a smooth one for the control, with a gradual increase in ganglion cell density with decreasing foveal distances. By contrast, the glaucomatous eye showed a marked reduction in densities from the lasered to the unlasered portions of the retina.

One large spot ( $\geq 200\text{-}\mu\text{m}$  diameter of ablated photoreceptors) was quantitatively analyzed by measuring nucleolar positions and creating two-dimensional reconstructions for each of 3 eyes with glaucoma. All 3 of these spots showed greater densities of ganglion cells than the surrounding retinas. In addition, a fourth large spot in the glaucomatous eye of monkey No. 1 was examined that

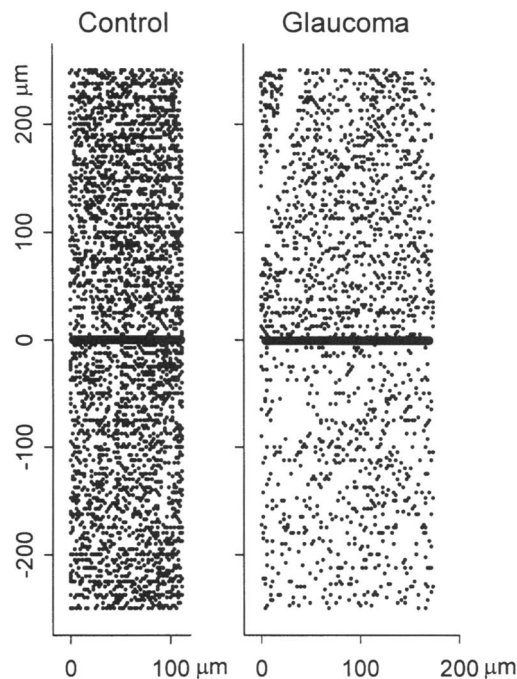


FIGURE 23

Two-dimensional reconstruction of ganglion cells over edge of 2 symmetrically placed, large, confluent laser spots in monkey No. 3. Positive numbers on left axis denote distances over burns. Thick lines mark edges of burns; no photoreceptors are present over burns (positive numbers). A distinct reduction in ganglion cell density is evident in eye with glaucoma but not in control eye. Larger distances along ordinates indicate decreasing foveal eccentricities.

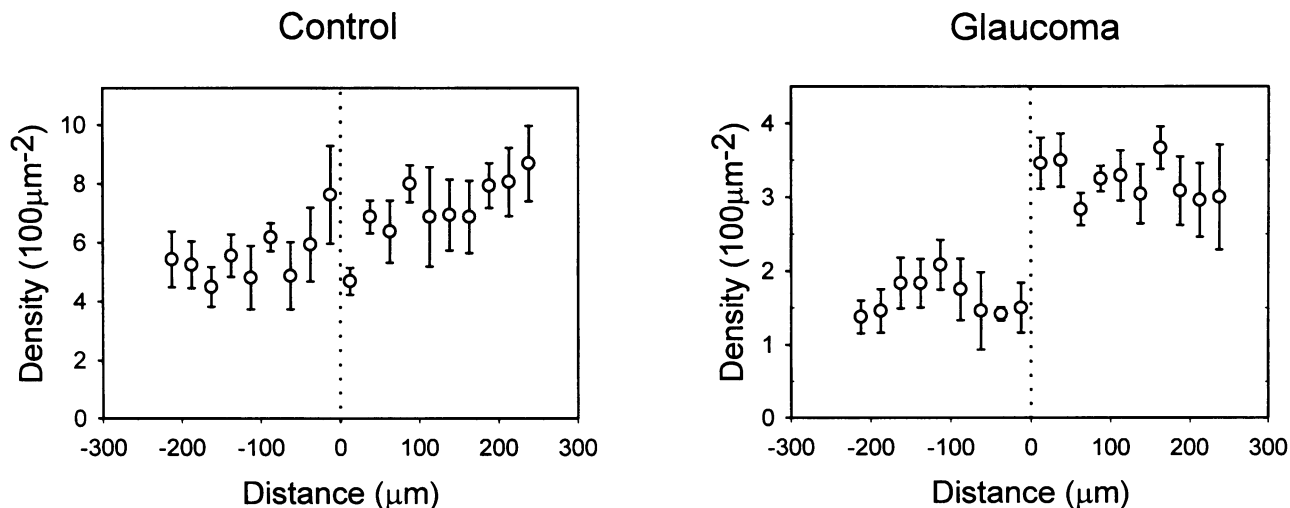


FIGURE 24

Plots of average ganglion cell density as function of foveal eccentricity. Positive numbers (to right of dotted lines) indicate ganglion cells overlying laser spots (destroyed photoreceptors). Larger positive distances represent decreasing foveal eccentricity. Bars denote SEM.



subjectively appeared to have a greater RGC density than the surrounding retina (Fig 21). Several small spots ( $\leq 100 \mu\text{m}$ ) were visually inspected in all of the glaucomatous eyes. There was no qualitative increase in ganglion cells over these spots. Two-dimensional reconstructions were not made for the small spots.

Three large spots were also examined by nucleolar measurement and two-dimensional reconstruction in nonglaucomatous eyes. No difference in ganglion cell density was apparent compared with the surrounding retina (Fig 23 and Fig 25).

*Retinal Laser Photocoagulation Followed by Optic Nerve Transection.* Monkey No. 4 underwent retinal laser photocoagulation in both eyes followed 4 weeks later by ONT in the right eye. A fluorescein angiogram was performed 4 weeks after the ONT. This showed normal retinal blood flow, indicating that the site of the ONT had been posterior to the insertion of the central retinal artery and vein.

Five and one-half weeks after the transection, the eyes were enucleated and processed for histologic evaluation as described earlier. Symmetrically located large laser spots were removed from the eyes, embedded and serially sectioned. The locations of the RGC nucleoli were measured, and two-dimensional graphical reconstructions were made (Fig 25). In the control eye, the RGCs were neither increased nor decreased compared with the surrounding

retina. The same was true for the eye that had undergone ONT, except that the average density of RGCs was greatly reduced in all areas.

### Discussion

*Type of Cells Over Laser Spots.* Although a few cells had features consistent with macrophages, activated RPE cells, or glial cells, most of the cells present over the retinal laser spots were probably RGCs. They were located at the level of, and were continuous with, the adjacent RGC layer. Few cells were seen in the inner plexiform layer, which would not have been the case had a great number of other cells (eg, glial or RPE) migrated in from elsewhere. Furthermore, a similar concentration of cells was not found either over the laser spots in the control eyes or over the retinal laser spots in the eye with ONT—again suggesting that most of the cells over the laser spots in the glaucomatous eyes were not other cell types that might have formed or congregated as part of the wound healing process.

Morphologically, the cells resembled RGCs in that they had large round nuclei, prominent nucleoli, abundant cytoplasm, and metachromatic thionin staining consistent with Nissl substance. Although anatomically similar in appearance, displaced amacrine cells are far too rare at these eccentricities to account for the density of cells

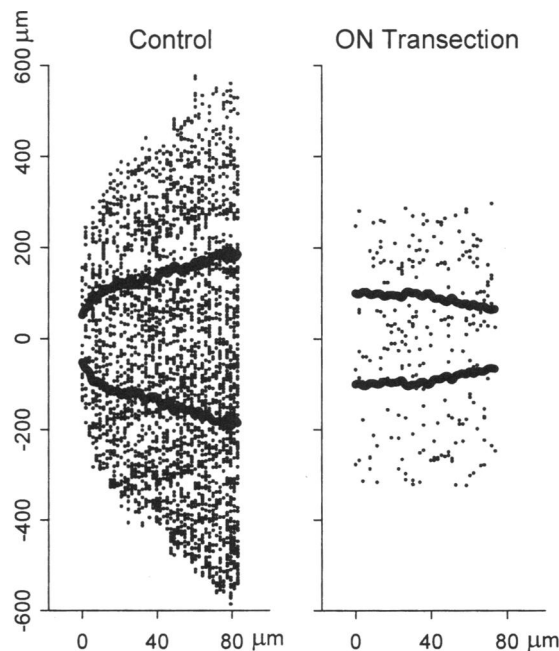


FIGURE 25

Two-dimensional reconstruction of ganglion cells over laser spots (no photoreceptors are present between thick lines) in a control eye and one that had undergone optic nerve transection approximately 1 month following laser application. Two eyes are from monkey No. 4. Both spots are located about 2.5 mm superonasal to foveal centers. Plots are oriented such that larger negative distances on ordinates are closest to foveas. There is no apparent change in density of ganglion cells seen over laser spots in either eye, although putative retinal ganglion cell density in eye with optic nerve transection is only about 10% of that in control eye. Bipolar cells are present in normal numbers over laser.

found.<sup>175</sup> Only a few cells in this layer had the spindle-shaped nuclei or contained cytoplasmic pigment granules characteristic of activated glial cells, RPE cells or macrophages. Also, the distribution of these cells seen on two-dimensional reconstruction was similar to (albeit of greater density than) the surrounding RGC layer (see large laser patch in Fig 23).

*Other Potential Causes of Altered RGC Density Over Laser Spots.* We cannot completely rule out some effect on the RGCs over the laser spots in the nonglaucomatous eyes. A few histologic sections of some of the spots appeared to have a subtle increase in RGC-like cells. However, when the positions of all nucleoli in all the cells with morphologic characteristics of RGCs were measured and plotted, no average increase in density was apparent (see controls in Figs 21, 23, and 25). The cause of this apparent increase in RGC concentration in some of the sections may have been due to normal random fluctuation, which is also seen over the nonlasered areas, or to slight shrinkage of the tissue over the laser spots. Increased RGC density has not been noted in the numerous publications describing the histologic features of laser spots in the eyes of either humans or monkeys.<sup>179</sup> In any event, the effect, if it exists, is small compared with the markedly higher RGC concentrations over the laser spots relative to the surrounding retinas seen in the glaucomatous eyes.

*Possible Mechanisms for the Protective Effect of Retinal Laser Photocoagulation in Glaucoma.*

1. Nonspecific protective effect. Although these results are predicted by the anterograde hypothesis, it is also possible that they could be due to some as yet unknown, nonspecific effect, not necessarily related to photoreceptor injury per se—such as thinning of the retina, which would allow more oxygen to reach the RGC layer from the choroid;<sup>160</sup> releasing of neurotrophic or neuroprotective factors, such as basic fibroblastic growth factor;<sup>151</sup> or by activating synthesis of heat shock proteins in the RGCs.<sup>134</sup> Activated retinal pigment epithelial cells, macrophages, or Müller cells could serve as mediators for these products. However, no protective effect was seen in the case of retinal laser photocoagulation preceding ONT. Therefore, a nonspecific effect, if there is one, is not sufficient to permit ganglion cell survival under these circumstances.

Owing to heat dissipation at the edges of the laser spots, the area of absent photoreceptors is smaller than the area of disturbed pigment in the RPE cells. This effect can be seen in Fig 18, where the diameter

of whitening of the original spot is about 500  $\mu\text{m}$  compared with a diameter of only about 250  $\mu\text{m}$  of photoreceptor destruction (this disparity is notable even considering the approximately 15% tissue shrinkage on embedment in glycol methacrylate). Yet the extent of this protection seems to be limited precisely to the region of photoreceptor destruction. This, too, is consistent with the hypothesis that RGC death is mediated specifically by photoreceptor injury and not the result of laser damage to the RPE. Similarly, we believe that the small laser spots killed too few photoreceptors to produce a measurable protective effect.

The presence or absence of bipolar cells in the laser spot does not seem to be critical in affecting protection of the RGCs. Furthermore, as noted previously, simply damaging the RPE cells without killing the photoreceptors is insufficient to protect the RGCs. Therefore, it may be that elimination of the photoreceptors is a critical aspect of the protective effect.

Finally, nonspecific forms of RGC neuroprotection have been observed in a rat model of ONT. Yip and associates<sup>152</sup> reported a preliminary study showing that a short period of low-level laser applied to the retina enhances RGC survival after optic nerve axotomy, and Di Polo and colleagues<sup>153</sup> showed that RGC death could be delayed by prolonged delivery of brain-derived neurotrophic factor. In both of these studies, the effects were transient, while our laser treatment provides a long-term (at least for the several months duration of these experiments) rescue in primates with experimental glaucoma. The differences between these studies could be accounted for by several factors. First, axotomy may be too damaging for any nonspecific neuroprotective environment to overcome. This is evidenced in part by failure of the retinal laser photocoagulation to prevent RGC death in the axotomized primate eye. Alternatively, the loss of photoreceptors would provide a permanent break in the anterograde chain of events that leads to RGC death in glaucomatous eyes (see next section), and we would predict that the protective effect would be permanent. Both these models are consistent with our results and warrant further study.

2. Interruption of the transsynaptic glutamate cascade. The protective effect on RGCs described here could be specific to a mechanism of RGC death in glaucomatous eyes, (ie, consistent with the anterograde hypothesis). One possible mechanism by which this could occur might be by interruption of the transsynaptic glutamate cascade between the photoreceptors and the RGCs. Elevated levels of glutamate have been

found in the vitreous body of eyes of humans and monkeys with glaucoma.<sup>167</sup> The source of this excess glutamate has not been demonstrated in glaucomatous eyes, although Yoles and Schwartz<sup>184</sup> showed that intraocular glutamate is increased in a rat model of optic nerve crush. However, considering that glutamate is the primary excitatory neurotransmitter of the photoreceptors and bipolar cells and that the outer retina shows signs of injury in glaucomatous eyes, this may be another possible source of the intravitreal glutamate. Although axonal injury can result in RGC death, these cells also contain NMDA glutamate receptors<sup>185</sup> and could possibly be damaged by chronically elevated glutamate levels.<sup>186,187</sup> Considering that the photoreceptors show signs of stress, which is perhaps the result of decreased choroidal blood flow that is known to occur with elevated IOP,<sup>142,145-150,188</sup> these injured cells might either release excess or fail to reuptake their glutamate. Increased levels of glutamate would, in turn, overstimulate the bipolar cells, which would release excess glutamate and thus chronically overexcite the RGCs.

We have shown that retinal laser photocoagulation protects the overlying RGCs for extended periods in experimental glaucoma. Whether these cells are functional remains to be elucidated. The precise mechanisms behind this phenomenon are not known. It may be due to nonspecific neuroprotective effects caused by the laser treatment or an interruption of a transsynaptic signal, which is toxic to RGCs originating from photoreceptors. Challenges remain to determine what the mechanism is and if it can be made applicable to the treatment of human glaucoma.

## **IMPLICATIONS FOR FUTURE RESEARCH AND TREATMENT**

---

### **ACQUIRED COLOR VISION LOSS**

In all 3 of the diseases discussed in this thesis—retinal detachment, diabetic retinopathy, and glaucoma—there is morphologic evidence for photoreceptor injury. For retinal detachment and diabetic retinopathy, there is specific loss of the blue-sensitive cones,—so it is easy to see how this would be either the sole factor or a contributing factor in acquired tritanopia (blue-yellow confusion). However, to understand how the L- and M-cone injury that was found in glaucoma could also result in a blue-yellow color discrimination deficit, 2 aspects of retinal physiology need to be considered. First, because of the spectral opponency mechanism, equal stimulation of the L- and M-cones is subjectively interpreted as “yellow.” Indeed, the Nagel anomaloscope is based on this

principle. In this instrument, monochromatic yellow is presented to the subject, who then is asked to turn knobs that mix red and green light to match the yellow. If there is an abnormality (most often congenital) in either the L- or M-cone absorption spectrum, a match point would result that is different from that of the normal population. This could be due to a spectral shift (as in the deuteranomalies), an absent red or green spectrum (as in the deuteranopias), or an unequal reduction in amplitude (decreased quantum capture). However, if the reduction of the spectral amplitudes is equal for both the L- and M-pathways, then there would be no shift of the “yellow” but a decrease in sensitivity to yellow light (ie, a blue-yellow confusion).

The problem with this latter scenario is the seemingly unlikely possibility that a disease would affect 2 cell types (in this case, the L- and M-cones) to precisely the same degree. Yet this is not so unreasonable given that these 2 cone types are so similar in terms of their biochemistry. For example, there is a 96% similarity in the amino acid sequence of the 2 opsins.<sup>33</sup> It also is now known that the 2 opsins are not only encoded for on the same chromosome, but that they share the same promoter. Finally, recent work to distinguish the 2 cone types in the living human eye has confirmed what has long been suspected—that the distribution of the 2 cone types is identical and, in fact, random with respect to one another.<sup>189</sup> So even if a disorder affected different parts of the retina differentially, the L- and M-cones would likely be involved by precisely the same amount.

Of course, demonstrating injury to the photoreceptors does not mean that higher order pathways do not also contribute to acquired color vision loss. For example, Greenstein and coworkers<sup>41</sup> have described post-receptor sensitivity loss in diabetic retinopathy. Nevertheless, the nearly total loss of the S-cones in retinal detachment is sufficient to explain the spectral sensitivity loss in this disease. Furthermore, the observation that the L/M-cones seem to be more affected in glaucoma as contrasted with the specific S-cone loss in diabetic retinopathy is consistent with the finding of Greenstein and associates<sup>37</sup> of decreased sensitivity in the yellow (red plus green) pathway in glaucoma.

### **THE ANTEROGRADE HYPOTHESIS OF GLAUCOMA**

#### *Summary*

Contrary to prevailing thought, these morphologic studies suggest that glaucoma is not an exception to Köllner's rule of acquired color vision loss, (ie, there is, indeed, damage to the outer retina—specifically, apparently equal damage to the L- and M-cones). This injury to the L/M-cones could explain the blue-yellow color confusion typical of a

retinopathy as opposed to the red-green confusion seen in most primary optic neuropathies. Interestingly, unlike the situation in retinal detachment and diabetic retinopathy, where S-cones are lost, it is the L/M-cones that are injured in glaucoma. The L/M-cones are the dominant cone population, and most of the ganglion cells receive input from this population. Finally, the distribution of cone injury in glaucoma may first occur in the same arcuate region where ganglion cells are initially lost. On the basis of these and other observations, the possibility is raised that the cones may be contributing in some way to ganglion cell death in this disease. This is referred to as the “anterograde” hypothesis because a key feature of it is ganglion cell death mediated by upstream processes. (For a more detailed description, please see the previous section entitled “Anterograde Hypothesis of Ganglion Cell Death in Glaucoma.”)

The retrograde hypothesis (damage to the ganglion cell axons as they pass through the anterior optic nerve followed by retrograde degeneration of the cell bodies) is the generally accepted mechanism in moderate-and-low pressure glaucoma. The most significant aspect of the findings discussed in this thesis, along with the other studies cited showing outer retinal damage, is that they suggest that a previously unsuspected mechanism of ganglion cell destruction may be at work. Furthermore, the preliminary results with retinal laser ablation of the photoreceptors are consistent with an anterograde mechanism.

Another possibility is that both the anterograde and retrograde mechanisms work together to kill the ganglion cells in glaucoma. For example, either ischemic or vascular damage to the optic nerve alone may be insufficient to cause ganglion cell death in most cases, but when combined with overexcitation from the cones, the ganglion cells may be pushed beyond their compensatory ability.

#### *Implications for Future Research and Therapy*

Understanding the controlling mechanisms of any disease is obviously important to finding new and more effective therapies. Until now, good progress in glaucoma treatment has been made because most of the effort has gone into lowering intraocular pressure. Since elevated pressure is the initial event in the chain that leads to ganglion cell death, regardless of whether the anterograde or retrograde hypothesis is accountable, lowering of the pressure should be, and is, a highly effective treatment.

Pressure control, however, has its limitations. Often, even with the newer medications, an acceptable target pressure cannot be achieved that will prevent further ganglion cell loss. The clinician is then faced with employing invasive, and too often unsuccessful, procedures such as trabeculectomy, implantation of valves, or ablation of the ciliary epithelium.

Should photoreceptor-induced excitotoxicity be shown to be an important mechanism in this disease, there would be new possibilities for future therapies. For example, the choroidal vasculature is under control of the autonomic nervous system. Yamamoto and coworkers<sup>190</sup> found that in rats, ablating the pterygopalatine ganglion, which supplies the parasympathetic innervation to the choroid, resulted in a marked decrease of nitric oxide synthase (NOS) activity in the choroid. Its product, nitric oxide, is responsible for vasodilatation. To their surprise, the surgical procedure resulted in a marked increase in NOS production by the ganglion cells. Although they were uncertain as to why this occurred, it is consistent with the anterograde hypothesis.

Suppose drugs could be developed that would have the opposite effect? It might one day be possible to increase the choroidal blood flow pharmacologically in spite of the elevated IOP, thus breaking the chain of excitotoxicity and, as happened with laser ablation of the photoreceptors, allow the ganglion cells to survive much higher pressures. Used as an adjunct to pressure-lowering drugs, choroidal blood flow enhancers should have a synergistic effect, permitting the eye to tolerate a much higher target pressure.

This is only one possibility. Other drugs might be developed that would limit the release or enhance the reuptake of glutamate by the ischemic photoreceptors.

Even when pressure lowering is apparently successful, clinicians have long known that there can still be gradual deterioration of the visual field. Could it be that there is an unwanted side effect to some of these medications? For example, one of the most commonly used antiglaucoma drugs is the beta-adrenergic blocker timolol maleate. While highly effective as a pressure-lowering agent, it may also significantly reduce choroidal perfusion<sup>191-193</sup>—thus perhaps giving a false sense of security, since its pressure-lowering properties are the only ones commonly measured. Consistent with this idea, a few studies have prospectively compared the beta-selective blocker betaxolol with timolol, which is nonselective, and found at least some beneficial effect on peripheral visual function—*independent of intraocular pressure lowering*.<sup>194-197</sup>

Another illustration of the need for understanding disease mechanisms is the following: Work thus far seems to implicate specifically the L- and M-cones as the major players in the anterograde model. Interestingly, these are the only photoreceptors that contain carbonic anhydrase.<sup>26</sup> Carbonic anhydrase inhibitors are commonly employed in the treatment of glaucoma. What effect are these drugs having on the L/M-cones? Is it beneficial or harmful to inhibit their carbonic anhydrase?

The lowering of intraocular pressure has always served as a proxy for therapeutic efficacy in glaucoma.

Monitoring ganglion cell loss via visual field testing is untenable because significant field changes may take decades. Indeed, visual field testing probably corresponds most closely to the distribution of the dead ganglion cells—much like the odometer on an automobile indicates distance traveled. What is needed is a way to easily measure how rapidly the ganglion cells are dying at the time of testing—something more like a speedometer. If the anterograde mechanism eventually proves to be an important aspect of ganglion cell death in glaucoma, it may one day be possible to monitor the photoreceptors themselves, since they may respond dynamically to choroidal ischemia. Such a test might even detect the effects of glaucoma prior to ganglion cell death, while the disease is still in a reversible stage.

#### ACKNOWLEDGEMENTS

The author thanks the Lions Eye Bank of Wisconsin, Inc (Madison) and Ingolf H. L. Wallow, MD, for providing some of the human eyes and Charlene B. Y. Kim, PhD, for critically reviewing the manuscript. The author also acknowledges the assistance of Nam-Chun Cho, MD; Gretchen L. Poulsen; Robert W. Nickells, PhD; James N. Ver Hoeve, PhD; Leonard A. Levin, MD, PhD; Mark J. Lucarelli, MD; James V. Schoster, DVM.

#### REFERENCES

1. Köllner H. *Die Störungen des Farbensehens, ihre klinische Bedeutung und ihre Diagnose*. Berlin: Karger;1912:234-258.
2. Verriest G. Further studies on acquired deficiency of color discrimination. *J Opt Soc Am* 1963;53:185-195.
3. Marré M, Marré E. Different types of acquired colour vision deficiencies on the base of CVM patterns in dependence upon the fixation mode of the diseased eye. *Mod Probl Ophthalmol* 1978;19:248-252.
4. Birch J, Chisholm IA, Kinnear P, et al. Acquired color vision defects. In: Pokorny J, Smith VC, Verriest G, et al, eds. *Congenital and Acquired Color Vision Defects*. New York: Grune & Stratton; 1979:243-348.
5. Koliopoulos J, Theodosiadis G. Retinal detachment and acquired colour vision disturbance. *Mod Probl Ophthalmol* 1972;11:117-121.
6. Drum B, Armaly MF, Huppert WE. Sources of short wavelength sensitivity loss in glaucoma. *Doc Ophthalmol Proc Ser* 1987;46:413-422.
7. Gastaud P, Vola J, Saracco JB, et al. Diabetic dyschromatopsia. Pathogenic hypothesis. *Doc Ophthalmol Proc Ser* 1987;46:387-390.
8. Kinnear PR, Aspinall PA, Lakowski R. The diabetic eye and colour vision. *Trans Ophthalmol Soc UK* 1972;92:69-78.
9. Lakowski R, Aspinall PA, Kinnear PR. Association between colour vision losses and diabetes mellitus. *Ophthalmol Res* 1973;4:145-149.
10. Marmor MF, Kessler R. Sildenafil (Viagra) and ophthalmology. *Surv Ophthalmol* 1999;44:153-162.
11. Marmor MF. Sildenafil (Viagra) and ophthalmology. *Arch Ophthalmol* 1999;117:518-519.
12. Hood DC, Benimoff WI, Greenstein VC. The response range of the blue-cone pathways. A source of vulnerability to disease. *Invest Ophthalmol Vis Sci* 1984;25:864-867.
13. Gündüz K, Arden GB, Perry S, et al. Color vision defects in ocular hypertension and glaucoma. Quantification with a computer-driven color television system. *Arch Ophthalmol* 1988;106:929-935.
14. Mollon JD. What is odd about the short-wavelength mechanism and why is it disproportionately vulnerable to acquired damage? Report of a discussion. *Doc Ophthalmol Proc Ser* 1983;33:145-149.
15. Farnsworth D. Tritanomalous vision as a threshold function. *Farbe* 1955;4:185-197.
16. Greenstein V, Hood DC, Campbell CJ. The use of a flash-on-flash paradigm to assess sensitivity changes due to retinal disease. *Invest Ophthalmol Vis Sci* 1982;23:102-112.
17. Hart WMJ, Burde RM. Three-dimensional topography of the central visual field. Sparing of foveal sensitivity in macular disease. *Ophthalmol* 1983;90:1028-1038.
18. Hart WMJ. Color contrast perimetry. Hue discrimination defects in acquired dyschromatopsias. *Doc Ophthalmol Proc Ser* 1987;46:267-273.
19. Hart WMJ. Acquired dyschromatopsias. *Surv Ophthalmol* 1987;32:10-31.
20. Osterberg GA. Topology of the layer of rods and cones in the human retina. *Acta Ophthalmol (Suppl)* 1935;6:1-103.
21. Marc RE, Sperling HG. Chromatic organization of primate cones. *Science* 1977;196:454-456.
22. Sperling HG, Johnson C, Harwerth RS. Differential spectral photic damage to primate cones. *Vision Res* 1980;20:1117-1125.
23. de Monasterio FM, Schein SJ, McCrane EP. Staining of blue-sensitive cones of the macaque retina by a fluorescent dye. *Science* 1981;213:1278-1281.
24. de Monasterio FM, McCrane EP, Newlander JK, et al. Density profile of blue-sensitive cones along the horizontal meridian of macaque retina. *Invest Ophthalmol Vis Sci* 1985;26:289-302.
25. Ahnelt PK, Kolb H, Pflug R. Identification of a subtype of cone photoreceptor, likely to be blue sensitive, in the human retina. *J Comp Neurol* 1987;255:18-34.
26. Nork TM, McCormick SA, Chao GM, et al. Distribution of carbonic anhydrase among human photoreceptors. *Invest Ophthalmol Vis Sci* 1990;31:1451-1458.
27. Silverman SE, Hart W, Jr, Gordon MO, et al. The dyschromatopsia of optic neuritis is determined in part by the foveal/perifoveal distribution of visual field damage. *Invest Ophthalmol Vis Sci* 1990;31:1895-1902.
28. McCrane EP, de Monasterio FM, Schein SJ, et al. Non-fluorescent dye staining of primate blue cones. *Invest Ophthalmol Vis Sci* 1983;24:1449-1455.
29. Zrenner E, Gouras P. Blue-sensitive cones of the cat produce a rod-like electroretinogram. *Invest Ophthalmol Vis Sci* 1979;18:1076-1081.
30. Hurvich LM, Jameson D. Some quantitative aspects of an opponent-colors theory. II. Brightness, saturation, and hue in normal and dichromatic vision. *J Opt Soc Am* 1955;45:602-616.
31. Derrington AM, Krauskopf J, Lennie P. Chromatic mechanisms in lateral geniculate nucleus of macaque. *J Physiol (Lond)* 1984;357:241-265.
32. Shapley RM, Hawken ML. Parallel retino-cortical channels and luminance. In: Gegenfurtner KR, Lindsay TS, eds. *Color Vision: From Genes to Perception*. Cambridge, UK: Cambridge University Press;1999:219-234.
33. Nathans J, Thomas D, Hogness DS. Molecular genetics of human color vision: The genes encoding blue, green and red pigments. *Science* 1986;232:193-202.

34. Szél Á, Takács L, Monostori É, et al. Monoclonal antibody-recognizing cone visual pigment. *Exp Eye Res* 1986;43:871-883.
35. Johnson LV, Hageman GS. Characterization of molecules bound by the cone photoreceptor-specific monoclonal antibody CSA-1. *Invest Ophthalmol Vis Sci* 1988;29:550-557.
36. Nork TM, Mangini NJ, Millecchia LL. Rods and cones contain antigenically distinctive S-antigens. *Invest Ophthalmol Vis Sci* 1993;34:2918-2925.
37. Greenstein VC, Shapiro A, Hood DC, et al. Chromatic and luminance sensitivity in diabetes and glaucoma. *J Opt Soc Am A* 1993;10:1785-1791.
38. Seiple WH, Holopigian K, Greenstein VC, et al. Sites of cone system sensitivity loss in retinitis pigmentosa. *Invest Ophthalmol Vis Sci* 1993;34:2638-2645.
39. Milam AH, Jacobson SG. Photoreceptor rosettes with blue cone opsin immunoreactivity in retinitis pigmentosa. *Ophthalmol* 1990;97:1620-1631.
40. Swanson WH, Birch DG, Anderson JL. S-cone function in patients with retinitis pigmentosa. *Invest Ophthalmol Vis Sci* 1993;34:3045-3055.
41. Greenstein VC, Shapiro A, Zaidi Q, et al. Psychophysical evidence for post-receptor sensitivity loss in diabetics. *Invest Ophthalmol Vis Sci* 1992;33:2781-2790.
42. Köllner H. Untersuchungen über die Farbenstörung bei Netzhautablösung. *Zeitschr Augenheilkd.* 1907;17:117-121.
43. Martin M, Menezo JC, Lopez H. Alterations in colour vision in patients operated on for retinal detachment. *Arch Soc Zsp Ophthalmol* 1972;32:793-808.
44. Chisholm A, McClure E, Foulds WS. Functional recovery of the retina after retinal detachment. *Trans Ophthalmol Soc UK* 1975;95:167-172.
45. Marré M. The investigation of acquired colour vision deficiencies. In: International Colour Association, ed. *Colour 73* London: Hilger;1973:99-135.
46. Barca L, De Luca A, Passani F. Color discrimination (100-hue test) after successful surgical treatment of retinal detachment. *Doc Ophthalmol Proc Ser* 1985;39:349-353.
47. Gundry MF, Davies EWG. Recovery of visual acuity after retinal detachment surgery. *Am J Ophthalmol* 1974;77:310-314.
48. Gruposso SS. Visual acuity following surgery for retinal detachment. *Arch Ophthalmol* 1975;93:327-330.
49. Burton TC. Recovery of visual acuity after retinal detachment involving the macula. *Tr Am Ophthalmol Soc* 1982;80:475-497.
50. Kroll AJ, Macherer R. Experimental retinal detachment in the owl monkey. III. Electron microscopy of retina and pigment epithelium. *Am J Ophthalmol* 1968;66:410-427.
51. Anderson DH, Guerin CJ, Erickson PA, et al. Morphological recovery in the reattached retina. *Invest Ophthalmol Vis Sci* 1986;27:168-183.
52. Guérin CJ, Anderson DH, Fariss RN, et al. Retinal reattachment of the primate macula. Photoreceptor recovery after short-term detachment. *Invest Ophthalmol Vis Sci* 1989;30:1708-1725.
53. Nork TM, Millecchia LL, Strickland BD, et al. Selective loss of blue cones and rods in human retinal detachment. *Arch Ophthalmol* 1995;113:1066-1073.
54. Donner K, Hemila S, Kalamkarov G, et al. Rod phototransduction modulated by bicarbonate in the frog retina: roles of carbonic anhydrase and bicarbonate exchange. *J Physiol (London)* 1990;426:297-316.
55. Lewis GP, Guérin CJ, Anderson DH, et al. Rapid changes in the expression of glial cell proteins caused by experimental retinal detachment. *Am J Ophthalmol* 1994;118:368-376.
56. Lewis GP, Erickson PA, Guerin CJ, Anderson DH, Fisher SK. Changes in the expression of specific Müller cell proteins during long-term retinal detachment. *Exp Eye Res* 1989;49:93-111.
57. Diabetic Retinopathy Study Research Group. Photocoagulation treatment of diabetic retinopathy. Clinical application of diabetic retinopathy study (DRS) findings. DRS report No. 8. *Ophthalmol* 1981;88:583-600.
58. Adams AJ, Zisman F, Ai E, et al. Macular edema reduces B cone sensitivity in diabetics. *Appl Optics* 1987;26:1455-1457.
59. Greenstein VC, Hood DC, Ritch R, et al. S (blue) cone pathway vulnerability in retinitis pigmentosa, diabetes and glaucoma. *Invest Ophthalmol Vis Sci* 1989;30:1732-1737.
60. Greenstein V, Sarter B, Hood D, et al. Hue discrimination and S cone pathway sensitivity in early diabetic retinopathy. *Invest Ophthalmol Vis Sci* 1990;31:1008-1014.
61. Mantyjarvi M. Colour vision and dark adaptation in diabetic patients after photocoagulation. *Acta Ophthalmol* 1989;67:113-118.
62. Greenstein VC, Thomas SR, Blaustein H, et al. Effects of early diabetic retinopathy on rod system sensitivity. *Optom Vis Sci* 1993;70:18-23.
63. Adams AJ. Chromatic and luminosity processing in retinal disease. *Am J Optom Physiol Opt* 1982;59:954-960.
64. Zisman F, Adams AJ. Spectral sensitivity of cone mechanisms in juvenile diabetics. *Doc Ophthalmol Proc Ser* 1983;33:127-131.
65. Roy MS, Gunkel RD, Podgor MJ. Color vision defects in early diabetic retinopathy. *Arch Ophthalmol* 1986;104:225-228.
66. Moloney J, Drury MI. Retinopathy and retinal function in insulin-dependent diabetes mellitus. *Br J Ophthalmol* 1982;66:759-761.
67. Bresnick GH, Condit RS, Palta M, et al. Association of hue discrimination loss and diabetic retinopathy. *Arch Ophthalmol* 1985;103:1317-1324.
68. Birch-Cox J. Defective colour vision in diabetic retinopathy before and after laser photocoagulation. *Mod Probl Ophthalmol* 1978;19:326-329.
69. Rockett M, Anderle D, Bessman AN. Blue-yellow vision defects in patients with diabetes. *West J Med* 1987;146:431-433.
70. Birch J. Colour vision changes following different types and amounts of argon laser photocoagulation in the treatment of diabetic retinopathy. *Doc Ophthalmol Proc Ser* 1987;46:31-36.
71. Lutze M, Bresnick GH. Lenses of diabetic patients "yellow" at an accelerated rate similar to older normals. *Invest Ophthalmol Vis Sci* 1991;32:194-199.
72. Terasaki H, Hirose H, Miyake Y. S-cone pathway sensitivity in diabetes measured with threshold versus intensity curves on flashed backgrounds. *Invest Ophthalmol Vis Sci* 1996;37:680-684.
73. Tregear SJ, Knowles PJ, Ripley LG, et al. Chromatic-contrast threshold impairment in diabetes. *Eye* 1997;11:537-546.
74. Holopigian K, Greenstein VC, Seiple W, et al. Evidence for photoreceptor changes in patients with diabetic retinopathy. *Invest Ophthalmol Vis Sci* 1997;38:2355-2365.
75. Gavioli Y, Sherman Y, Ben-Sasson SA. Identification of programmed cell death in situ via specific labeling of nuclear DNA fragmentation. *J Cell Biol* 1992;119:493-501.
76. Chang GQ, Hao Y, Wong F. Apoptosis: Final common pathway of photoreceptor death in rd, rds, and rhodopsin mutant mice. *Neuron* 1993;11:595-605.
77. Ridderstrale Y. Intracellular localization of carbonic anhydrase in the frog nephron. *Acta Physiol Scand* 1976;98:465-469.
78. Hansson HPJ. Histochemical demonstration of carbonic anhydrase activity. *Histochemie* 1967;11:112-128.
79. Hansson HPJ. Histochemical demonstration of carbonic anhydrase activity in some epithelia noted for active transport. *Acta Physiol Scand* 1968;73:427-434.
80. Curcio CA, Sloan KR, Meyers D. Computer methods for sampling, reconstruction, display and analysis of retinal whole mounts. *Vision Res* 1989;29:529-540.
81. Nork TM, Ver Hoeve JN, Poulsen GL, et al. Swelling and loss of photoreceptors in chronic human and experimental glaucomas. *Arch Ophthalmol* 2000;118:235-245.

## Acquired Color Vision Loss and a Possible Mechanism of Ganglion Cell Death in Glaucoma

82. Becker B. Diabetes mellitus and primary open-angle glaucoma. The XXVII Edward Jackson Memorial Lecture. *Am J Ophthalmol* 1971;1:1-16.
83. Klein BE, Klein R, Jensen SC. Open-angle glaucoma and older-onset diabetes. The Beaver Dam Eye Study. *Ophthalmol* 1994;101:1173-1177.
84. Mitchell P, Smith W, Chey T, et al. Open-angle glaucoma and diabetes: the Blue Mountains eye study, Australia. *Ophthalmol* 1997;104:712-718.
85. Tielsch JM, Katz J, Singh K, et al. A population-based evaluation of glaucoma screening: The Baltimore Eye Survey. *Am J Epidemiol* 1991;134:1102-1110.
86. Jonas JB, Grundler AE. Prevalence of diabetes mellitus and arterial hypertension in primary and secondary open-angle glaucomas. *Graefes Arch Clin Exp Ophthalmol* 1998;236:202-206.
87. Garcia-Valenzuela E, Gorczyca W, Darzynkiewicz Z, et al. Apoptosis in adult retinal ganglion cells after axotomy. *J Neurobiol* 1994;25:431-438.
88. Didenko VV, Hornsby PJ. Presence of double-strand breaks with single-base 3' overhangs in cells undergoing apoptosis but not necrosis. *J Cell Biol* 1996;135:1369-1376.
89. Hidayat AA, Fine BS. Diabetic choroidopathy. Light and electron microscopic observations of 7 cases. *Ophthalmol* 1985;92:512-522.
90. Cao J, McLeod S, Merges CA, et al. Choriocapillaris degeneration and related pathologic changes in human diabetic eyes. *Arch Ophthalmol* 1998;116:589-597.
91. Kurtenbach A, Rüttiger L, Schiefer U, et al. Heterochromatic brightness matching and wavelength discrimination in juvenile diabetics: A 3-year study. In: Drum B, ed. *Colour Vision Deficiencies XII*. Dordrecht, the Netherlands: Kluwer Academic Publishers; 1995:47-52.
92. Hardy KJ, Lipton J, Scase MO, et al. Detection of colour vision abnormalities in uncomplicated type 1 diabetic patients with angiographically normal retinas. *Br J Ophthalmol* 1992;76:461-464.
93. Kurtenbach A, Schiefer U, Neu A, et al. Preretinopic changes in the colour vision of juvenile diabetics. *Br J Ophthalmol* 1999;83:43-46.
94. Quigley HA, Nickells RW, Kerrigan LA, et al. Retinal ganglion cell death in experimental glaucoma and after axotomy occurs by apoptosis. *Invest Ophthalmol Vis Sci* 1995;36:774-786.
95. Nickells RW. Apoptosis of retinal ganglion cells in glaucoma: an update of the molecular pathways involved in cell death. *Surv Ophthalmol* 1999;43 Suppl 1:S151-161.
96. Elschnig A. Chapter 11. In: Henke F, Lubarsch O, ed. *Handbuch der Speziellen Pathologischen Anatomie und Histologie*. Berlin: Springer; 1928:873.
97. Hayreh SS. Blood supply of the optic nerve head and its role in optic atrophy, glaucoma, and oedema of the optic disc. *Br J Ophthalmol* 1969;53:721-748.
98. Quigley HA, Green WR. The histology of human glaucoma cupping and nerve damage. Clinicopathologic correlation in 21 eyes. *Ophthalmol* 1979;10:1803-1827.
99. François J, Verriest G. Les dyschromatopsies acquises dans le glaucome primaire. *Ann Oculistique* 1959;192:191-199.
100. Grutznher P, Schleicher S. Acquired color vision defects in glaucoma patients. *Mod Probl Ophthalmol* 1972;11:136-140.
101. Fishman GA, Krill AE, Fishman M. Acquired color vision defects in patients with open-angle glaucoma and ocular hypertension. *Mod Probl Ophthalmol* 1974;13:335-338.
102. Lakowski R, Drance SM. Acquired dyschromatopsias. The earliest functional losses in glaucoma. *Doc Ophthalmol Proc Ser* 1979;19:159-165.
103. Poinosawmy D, Nagasubramanian S, Gloster J. Color vision in patients with chronic simple glaucoma and ocular hypertension. *Br J Ophthalmol* 1980;64:852-857.
104. Quigley HA, Addicks EM, Green RW. Optic nerve damage in human glaucoma. III. Quantitative correlation of nerve fiber loss and visual field defect in glaucoma, ischemic neuropathy, papilledema, and toxic neuropathy. *Ophthalmol* 1982;100:135-146.
105. Morrison JC, Dorman-Pease ME, Dunkelberger GR, et al. Optic nerve head extracellular matrix in primary optic atrophy and experimental glaucoma. *Arch Ophthalmol* 1990;108:1020-1024.
106. Quigley HA, Addicks EM. Regional differences in the structure of the lamina cribrosa and their relation to glaucomatous optic nerve damage. *Arch Ophthalmol* 1981;99:137-143.
107. Quigley HA, Addicks EM, Green WR, et al. Optic nerve damage in human glaucoma. II. The site of injury and susceptibility to damage. *Arch Ophthalmol* 1981;99:635-649.
108. Quigley HA, Sanchez RM, Dunkelberger GR, et al. Chronic glaucoma selectively damages large optic nerve fibers. *Invest Ophthalmol Vis Sci* 1987;28:913-920.
109. Quigley HA, Dunkelberger GR, Green WR. Chronic human glaucoma causing selectively greater loss of large optic nerve fibers. *Ophthalmol* 1988;95:357-363.
110. de Monasterio FM. Asymmetry of on- and off-pathways of blue-sensitive cones of the retina of macaques. *Brain Res* 1979;166:39-48.
111. Gouras P. Identification of cone mechanisms in monkey ganglion cells. *J Physiol* 1968;199:533-547.
112. Kaplan E, Shapley RM. The primate retina contains 2 types of ganglion cells, with high and low contrast sensitivity. *Proc Nat Acad Sci USA* 1986;83:2755-2757.
113. Nork TM, Cho NC, Poulsen GL. Selective loss of blue cones in human diabetic retinopathy. *Invest Ophthalmol Vis Sci* 1999;40(4):ARVO abstract no. 1618.
114. Anderson DR, Davis EB. Sensitivities of ocular tissues to acute pressure-induced ischemia. *Arch Ophthalmol* 1975;93:267-274.
115. Büchi ER. Cell death in the rat retina after a pressure-induced ischaemia-reperfusion insult: an electron microscopic study. I. Ganglion cell layer and inner nuclear layer. *Exp Eye Res* 1992;55:605-613.
116. Büchi ER. Cell death in rat retina after pressure-induced ischaemia-reperfusion insult: electron microscopic study. II. Outer nuclear layer. *Jpn J Ophthalmol* 1992;36:62-68.
117. Panda S, Jonas JB. Decreased photoreceptor count in human eyes with secondary angle-closure glaucoma. *Invest Ophthalmol Vis Sci* 1992;33:2532-2536.
118. Janssen P, Naskar R, Moore S, et al. Evidence for glaucoma-induced horizontal cell alterations in the human retina. *Ger J Ophthalmol* 1997;5:378-385.
119. Kendell KR, Quigley HA, Kerrigan LA, et al. Primary open-angle glaucoma is not associated with photoreceptor loss. *Invest Ophthalmol Vis Sci* 1995;36:200-205.
120. Wygnanski T, Desatnik H, Quigley HA, et al. Comparison of ganglion cell loss and cone loss in experimental glaucoma. *Am J Ophthalmol* 1995;120:184-189.
121. Alvis DL. Electroretinographic changes in controlled chronic open-angle glaucoma. *Am J Ophthalmol* 1966;61:121-131.
122. Fazio DT, Heckenlively JR, Martin DA, et al. The electroretinogram in advanced open-angle glaucoma. *Doc Ophthalmol* 1986;63:45-54.
123. Holopigian K, Seiple W, Mayron C, et al. Electrophysiological and psychophysical flicker sensitivity in patients with primary open-angle glaucoma and ocular hypertension. *Invest Ophthalmol Vis Sci* 1990;31:1863-1868.
124. Odom JV, Feghali JG, Jin JC, et al. Visual function deficits in glaucoma. Electroretinogram pattern and luminance nonlinearities. *Arch Ophthalmol* 1990;108:222-227.

125. Vaegan, Graham SL, Goldberg I, et al. Flash and pattern electroretinogram changes with optic atrophy and glaucoma. *Exp Eye Res* 1995;60:697-706.
126. Weiner A, Ripkin DJ, Patel S, et al. Foveal dysfunction and central visual field loss in glaucoma. *Arch Ophthalmol* 1998;116:1169-1174.
127. Frishman LJ, Shen FF, Du L, et al. The scotopic electroretinogram of macaque after retinal ganglion cell loss from experimental glaucoma. *Invest Ophthalmol Vis Sci* 1996;37:125-141.
128. Nork TM, Wang LP, Poulsen GL. Selective loss of photoreceptors in human diabetic retinopathy. *Invest Ophthalmol Vis Sci* 1994;35(4):S1588. ARVO abstract no. 1537.
129. Ogiso M. Examination of confusion loci in acquired color vision deficiency with surface color. *Nippon Ganka Gakkai Zasshi* 1993;97:411-418.
130. Greenstein VC, Halevy D, Zaidi Q, et al. Chromatic and luminance systems deficits in glaucoma. *Vision Res* 1996;36:621-629.
131. Kalloniatis M, Harwerth RS, Smith ELd, et al. Colour vision anomalies following experimental glaucoma in monkeys. *Ophthalmic Physiol Opt* 1993;13:56-67.
132. Röhrenbeck J, Wässle H, Boycott BB. Horizontal cells in the monkey retina: Immunocytochemical staining with antibodies against calcium binding proteins. *Eur J Neurosci* 1989;1:407-420.
133. Röhlich P, Szel A, Johnson LV, et al. Carbohydrate components recognized by the cone-specific monoclonal antibody CSA-1 and by peanut agglutinin are associated with red and green-sensitive cone photoreceptors. *J Comp Neurol* 1989;289:395-400.
134. Poulsen GL, Schlamp CL, Nork TM, et al. Changes in photoreceptor gene expression in glaucoma. *Invest Ophthalmol Vis Sci* 1999;40(4):S788. ARVO abstract no. 4148.
135. Ver Hoeve JN, Murdock TJ, Heatley GA, et al. Increased latency of early multifocal ERG response in glaucoma. *Invest Ophthalmol Vis Sci* 2000;41(4):S520. ARVO abstract no. 2772.
136. Hood DC, Greenstein V, Frishman L, et al. Identifying inner retinal contributions to the human multifocal ERG. *Vision Res* 1999;39:2285-2291.
137. Hood DC, Frishman LJ, Viswanathan S, et al. Evidence for a ganglion cell contribution to the primate electroretinogram (ERG): effects of TTX on the multifocal ERG in macaque. *Vis Neurosci* 1999;16:411-416.
138. Hare W, Ton H, Woldemussie E, et al. Electrophysiological and histological measures of retinal injury in chronic ocular hypertensive monkeys. *Eur J Ophthalmol* 1999;9 Suppl 1:S30-33.
139. Graham SL, Klistorner A. Electrophysiology: a review of signal origins and applications to investigating glaucoma. *Aust N Z J Ophthalmol* 1998;26:71-85.
140. Vaegan, Buckland L. The spatial distribution of ERG losses across the posterior pole of glaucomatous eyes in multifocal recordings. *Aust N Z J Ophthalmol* 1996;24:28-31.
141. Hart WM, Jr., Becker B. The onset and evolution of glaucomatous visual field defects. *Ophthalmol* 1982;89:268-279.
142. Alm A, Bill A. Blood flow and oxygen extraction in the cat uvea at normal and high intraocular pressures. *Acta Physiol Scand* 1970;80:19-28.
143. Yancey CM, Linsenmeier RA. Oxygen distribution and consumption in the cat retina at increased intraocular pressure. *Invest Ophthalmol Vis Sci* 1989;30:600-611.
144. Yancey CM, Linsenmeier RA. The electroretinogram and choroidal PO<sub>2</sub> in the cat during elevated intraocular pressure. *Invest Ophthalmol Vis Sci* 1988;29:700-707.
145. Rojanapongpun P, Drance SM, Morrison BJ. Ophthalmic artery flow velocity in glaucomatous and normal subjects. *Br J Ophthalmol* 1993;77:25-29.
146. Michelson G, Groh MJ, Groh ME, et al. Advanced primary open-angle glaucoma is associated with decreased ophthalmic artery blood-flow velocity. *Ger J Ophthalmol* 1995;4:21-24.
147. Cellini M, Possati GL, Caramazza N, et al. Colour Doppler analysis of the choroidal circulation in chronic open-angle glaucoma. *Ophthalmologica* 1996;210:200-202.
148. Yamazaki Y, Drance SM. The relationship between progression of visual field defects and retrobulbar circulation in patients with glaucoma. *Am J Ophthalmol* 1997;124:287-295.
149. Butt Z, C OB, McKillop G, et al. Color Doppler imaging in untreated high- and normal-pressure open-angle glaucoma. *Invest Ophthalmol Vis Sci* 1997;38:690-696.
150. Kaiser HJ, Schoetza A, Stumpf D, et al. Blood-flow velocities of the extraocular vessels in patients with high-tension and normal-tension primary open-angle glaucoma. *Am J Ophthalmol* 1997;123:320-327.
151. Yin ZQ, Vaegan, Millar TJ, et al. Widespread choroidal insufficiency in primary open-angle glaucoma. *J Glaucoma* 1997;6:23-32.
152. Yoneya S, Tso MO. Angioarchitecture of the human choroid. *Arch Ophthalmol* 1987;105:681-687.
153. Fryczkowski AW, Sherman MD, Walker J. Observations on the lobular organization of the human choriocapillaris. *Int Ophthalmol* 1991;15:109-120.
154. Hayreh SS, Baines JA. Occlusion of the posterior ciliary artery. I. Effects on choroidal circulation. *Br J Ophthalmol* 1972;56:719-735.
155. Hayreh SS, Baines JA. Occlusion of the posterior ciliary artery. II. Chorio-retinal lesions. *Br J Ophthalmol* 1972;56:736-753.
156. Stern WH, Ernest JT. Microsphere occlusion of the choriocapillaris in rhesus monkeys. *Am J Ophthalmol* 1974;78:438-448.
157. Hayreh SS. In vivo choroidal circulation and its watershed zones. *Eye* 1990;4:273-289.
158. Vaegan, Yin ZQ, Beaumont P. Delayed choroidal filling across the posterior pole of glaucomatous eyes shown by fluorescein angiography. *Invest Ophthalmol Vis Sci* 1995;36(4):S965. ARVO abstract no. 4452.
159. Rosen ES, Boyd TA. New method of assessing choroidal ischemia in open-angle glaucoma and ocular hypertension. *Am J Ophthalmol* 1970;70:912-921.
160. Wallow IH. Repair of the pigment epithelial barrier following photocoagulation. *Arch Ophthalmol* 1984;102:126-135.
161. Wallow IH, Sponsel WE, Stevens TS. Clinicopathologic correlation of diode laser burns in monkeys. *Arch Ophthalmol* 1991;109:648-653.
162. Stone JL, Barlow WE, Humayun MS, et al. Morphometric analysis of macular photoreceptors and ganglion cells in retinas with retinitis pigmentosa. *Arch Ophthalmol* 1992;110:1634-1639.
163. Eisenfeld AJ, LaVail MM, LaVail JH. Assessment of possible transneuronal changes in the retina of rats with inherited retinal dystrophy: cell size, number, synapses, and axonal transport by retinal ganglion cells. *J Comp Neurol* 1984;223:22-34.
164. Hartveit E, Brandstatter JH, Sassoe-Pognetto M, et al. Localization and developmental expression of the NMDA receptor subunit NR2A in the mammalian retina. *J Comp Neurol* 1994;348:570-582.
165. Brandstatter JH, Hartveit E, Sassoe-Pognetto M, et al. Expression of NMDA and high-affinity kainate receptor subunit mRNAs in the adult rat retina. *Eur J Neurosci* 1994;6:1100-1112.
166. Siliprandi R, Canella R, Carmignoto G, et al. N-methyl-D-aspartate-induced neurotoxicity in the adult rat retina. *Vis Neurosci* 1992;8:567-573.
167. Dreyer EB, Zurakowski D, Schumer RA, et al. Elevated glutamate levels in the vitreous body of humans and monkeys with glaucoma. *Arch Ophthalmol* 1996;114:299-305.
168. Vorwerk CK, Lipton SA, Zurakowski D, et al. Chronic low-dose glutamate is toxic to retinal ganglion cells. Toxicity blocked by memantine. *Invest Ophthalmol Vis Sci* 1996;37:1618-1624.
169. Massey SC. Cell types using glutamate as a neurotransmitter in the vertebrate retina. *Prog Retinal Res* 1990;9:399-425.
170. Perry VH, Oehler R, Cowey A. Retinal ganglion cells that project to the dorsal lateral geniculate nucleus in the macaque monkey. *Neuroscience* 1984;12:1101-1123.
171. Rodieck RW. The primate retina. In: Steklis HD, Erwin J, ed.



## Acquired Color Vision Loss and a Possible Mechanism of Ganglion Cell Death in Glaucoma

- Neurosciences (Comparative Primate Biology)*. New York: Alan R Liss; 1988:203-278.
172. Gaasterland D, Kupfer C. Experimental glaucoma in the rhesus monkey. *Invest Ophthalmol Vis Sci* 1974;13:455-457.
  173. Quigley HA, Hohman RM. Laser energy levels for trabecular meshwork damage in the primate eye. *Invest Ophthalmol Vis Sci* 1983;24:1305-1307.
  174. Pederson JE, Gaasterland DE. Laser-induced primate glaucoma. I. Progression of cupping. *Arch Ophthalmol* 1984;102:1689-1692.
  175. Kaufman PL, Wallow IH. Minified diagnostic contact lenses for biomicroscopic examination and photocoagulation of the anterior and posterior segment in small primates (Letter). *Exp Eye Res* 1985;40:883-885.
  176. Peterson JA, Kiland JA, Croft MA, et al. Intraocular pressure measurement in cynomolgus monkeys. Tono-Pen versus manometry. *Invest Ophthalmol Vis Sci* 1996;37:1197-1199.
  177. Gonnering RS, Dortzbach RK, Erickson KA, et al. The cynomolgus monkey as a model for orbital research. II. Anatomic effects of lateral orbitotomy. *Curr Eye Res* 1984;3:541-555.
  178. Curcio CA, Allen KA. Topography of ganglion cells in human retina. *J Comp Neurol* 1990;300:5-25.
  179. Wallow IHL. Clinicopathologic correlation of retinal photocoagulation in the human eye. In: Weingeist TA, Sneed SR, eds. *Laser Surgery in Ophthalmology*. Norwalk, CT: Appleton & Lange; 1992:15-27.
  180. Diddie KR, Ernest JT. The effect of photocoagulation on the choroidal vasculature and retinal oxygen tension. *Am J Ophthalmol* 1977;84:62-66.
  181. Xiao M, Sastry SM, Li ZY, et al. Effects of retinal laser photocoagulation on photoreceptor basic fibroblast growth factor and survival. *Invest Ophthalmol Vis Sci* 1998;39:618-630.
  182. Yip HK, Lam LW, So KF. Short period of low level laser enhances retinal ganglion cell (RGC) survival after optic nerve axotomy in adult SD rats. *Invest Ophthalmol Vis Sci* 1999;40(4):S132. ARVO Abstract.
  183. Di Polo A, Aigner LJ, Dunn RJ, et al. Prolonged delivery of brain-derived neurotrophic factor by adenovirus-infected Muller cells temporarily rescues injured retinal ganglion cells. *Proc Natl Acad Sci U S A*. 1998;95:3978-3983.
  184. Yoles E, Schwartz M. Elevation of intraocular glutamate levels in rats with partial lesion of the optic nerve. *Arch Ophthalmol* 1998;116:906-910.
  185. Watanabe M, Mishina M, Inoue Y. Differential distributions of the NMDA receptor channel subunit mRNAs in the mouse retina. *Brain Res* 1994;634:328-332.
  186. Dreyer EB, Zhang D, Lipton SA. Transcriptional or translational inhibition blocks low dose NMDA-mediated cell death. *Neuroreport* 1995;6:942-944.
  187. Otori Y, Wei JY, Barnstable CJ. Neurotoxic effects of low doses of glutamate on purified rat retinal ganglion cells. *Invest Ophthalmol Vis Sci* 1998;39:972-981.
  188. Alm A, Bill A. Ocular and optic nerve blood flow at normal and increased intraocular pressures in monkeys (*Macaca irus*): A study with radioactively labelled microspheres including flow determinations in brain and some other tissues. *Exp Eye Res* 1973;15:15-29.
  189. Roorda A, Williams DR. The arrangement of the 3 cone classes in the living human eye. *Nature* 1999;397:520-522.
  190. Yamamoto R, Brecht DS, Dawson TM, et al. Enhanced expression of nitric oxide synthase by rat retina following pterygopalatine parasympathetic denervation. *Brain Res* 1993;631:83-88.
  191. Baxter GM, Williamson TH, McKillop G, et al. Color Doppler ultrasound of orbital and optic nerve blood flow: effects of posture and timolol 0.5%. *Invest Ophthalmol Vis Sci* 1992;33:604-610.
  192. Chiou GC, Chen YJ. Effects of antiglaucoma drugs on ocular blood flow in ocular hypertensive rabbits. *J Ocul Pharmacol* 1993;9:13-24.
  193. Millar JC, Wilson WS, Carr RD, et al. Drug effects on intraocular pressure and vascular flow in the bovine perfused eye using radio-labelled microspheres. *J Ocul Pharmacol Ther* 1995;11:11-23.
  194. Collignon-Brach J. Longterm effect of topical beta-blockers on intraocular pressure and visual field sensitivity in ocular hypertension and chronic open-angle glaucoma. *Surv Ophthalmol* 1994;38 Suppl:S149-155.
  195. Kaiser HJ, Flammer J, Stumpf D, et al. Longterm visual field follow-up of glaucoma patients treated with beta-blockers. *Surv Ophthalmol* 1994;38 Suppl:S156-159; discussion S160.
  196. Drance SM. A comparison of the effects of betaxolol, timolol, and pilocarpine on visual function in patients with open-angle glaucoma. *J Glaucoma* 1998;7:247-252.
  197. Vainio-Jylha E, Vuori ML. The favorable effect of topical betaxolol and timolol on glaucomatous visual fields: a 2-year follow-up study. *Graefes Arch Clin Exp Ophthalmol* 1999;237:100-104.